Environmental Challenges 5 (2021) 100284

Contents lists available at ScienceDirect

Environmental Challenges

journal homepage: www.elsevier.com/locate/envc

Investigation on thermal properties of rice husk ash-blended palm kernel shell concrete

A.A. RAHEEM[a], K.O. ORIOLA[b], M.A. KAREEM[c,*], R. ABDULWAHAB[d]

[a] Department of Civil Engineering, Ladoke Akintola University of Technology, Ogbomoso, Nigeria
[b] Department of Agricultural Engineering, Ladoke Akintola University of Technology, Ogbomoso, Nigeria
[c] Department of Civil Engineering, Osun State University, Osogbo, Nigeria
[d] Department of Civil and Environmental Engineering, Kwara State University, Malete, Nigeria

ARTICLE INFO

Keywords:
Concrete
Oven-dried density
Palm kernel shell
Rice husk ash
Thermal conductivity
Thermal diffusivity

ABSTRACT

The contribution of buildings to climate change as a result of energy consumption and greenhouse gas emissions necessitates the use of agro-industrial by-products as alternative construction materials. The present study examines the thermal properties of Rice husk ash-blended Palm Kernel Shell Concrete (RHA-blended PKSC). Three control concrete mixes with mix ratios of 1:1$\frac{1}{2}$:3, 1:2:4 and 1:3:6 using water-to-cement (w/c) ratios of 0.5, 0.6 and 0.7, respectively were made with cement, river sand and granite. For each mix ratio with the respective w/c ratio, five concrete mixes containing RHA fixed at 15% as replacement for cement and PKS at 20, 40, 60, 80 and 100% as replacement for crushed granite were produced. The oven-dry density, compressive strength and thermal properties (thermal conductivity, thermal diffusivity, volumetric heat capacity and thermal resistivity) were determined. The results showed that the oven-dry density and compressive strength of concrete declined with increasing PKS content. Nevertheless, the compressive strength increased with curing age and the gain in strength of RHA-blended PKSC were higher than the control at the later age. The thermal conductivity and diffusivity decreased with increasing PKS contents but increase with curing age while volumetric heat capacity and thermal resistivity increased as PKS content increases but decreased with curing age. In addition, concrete with 1:3:6 mix ratio exhibited the lowest thermal conductivity and diffusivity but higher volumetric heat capacity and thermal resistivity than those with 1:1$\frac{1}{2}$:3, 1:2:4 mix ratios. RHA-blended PKSC with 40% PKS and 15% RHA for 1:1$\frac{1}{2}$:3 mix ratio attained the compressive strength and thermal conductivity values recommended for lightweight aggregate concrete which is suitable for structural and insulation purposes. It was concluded that the combined use of PKS and RHA as raw materials in concrete is effective in improving concrete's thermal and insulation properties.

1. Introduction

Concrete is the most widely utilized construction material and its application is rank third behind air and water (CEMBUREAU, 2020). The component used for concrete production are sand, granite, water with or without admixture. One of the vital requirements of a structure is the provision of thermal comfort and reduction of energy consumption (Reddy et al., 2020). The increase in energy demand from buildings can be attributed to the inability of the conventional building materials to satisfy the thermal comfort requirements for its occupants (IEA, 2020). According to Thakur et al., (2020), the atmosphere within a building is mainly determined by how heat, moisture, and wind interact with the building's envelope and the surrounding environment. The CO_2 emissions resulting from electricity and non-renewable energy sources for the provision of thermal comfort in building rose to 10 Gt in 2019 (IEA, 2020). With rising air conditioning possession and climate change, the need for heating and cooling accounts for more than one-third of global final energy consumption and nearly 40% of direct and indirect CO_2 emissions. Thermal properties of building materials can be improved to reduce building energy consumption (Shafigh et al., 2018).

The knowledge of the thermal properties of the structure components is critical in the assessment of the thermal efficiency of a system (Misri et al., 2018). Thermal conductivity, thermal diffusivity, thermal resistivity, and specific heat are the thermo-physical parameters used to evaluate the thermal behavior of concrete. Thermal conductivity is a property which determines the capacity of a material to conduct and accumulate heat (Aurangzeb et al., 2006). Thermal diffusivity is a parameter which governs how quickly temperature changes within

* Corresponding author.
E-mail address: mutiu.kareem@uniosun.edu.ng (M.A. KAREEM).

https://doi.org/10.1016/j.envc.2021.100284
Received 27 July 2021; Received in revised form 10 September 2021; Accepted 10 September 2021
2667-0100/© 2021 The Author(s). Published by Elsevier B.V. This is an open access article under the CC BY license (http://creativecommons.org/licenses/by/4.0/)

a mass may pass through a medium, thus, it can be used to measure how well concrete can withstand temperature changes (Howlader et al., 2012). Thermal resistivity is a property that determines a material's thermal transport capability and is an indicator of its insulative efficiency (Howlader et al., 2012). The specific heat is a measures of the quantity of energy requires to raise a unit mass's temperature by one degree. (Shafigh et al., 2018). Heat transfer and energy consumption in buildings are limited by concrete with low thermal conductivity (Asadi et al., 2019). The thermal conductivity of concrete depends on concrete density, aggregate types, shape and packing type, and moisture content (Misri et al., 2018; Aurangzeb et al., 2006; Kodur and Sultan, 2003; ACI 122R-14 2014). Lightweight aggregates (LWAs) are generally considered as materials with better insulating and thermal properties (Thakur et al., 2020; Sengul et al., 2011). Aggregate with bulk density ranging from 500 to 1120 kg/m^3 are generally known as LWA while those with bulk density between 1520 and 1680 kg/m^3 are known as normal aggregate (NA) (Li, 2011). Several investigations have indicated that adding LWAs to concrete reduces the thermal conductivity of the material (Aurangzeb et al., 2006; Demirboga and Gül, 2003). In past few decades, there has been growing interest in using agricultural and industrial by-products as a substitute for reducing the continuous use of NA, which is the most abundant components in concrete (Skalny et al., 2002). Numerous studies have established the potentials of using agricultural residues as LWAs for improving the thermal and insulation properties in lightweight concrete production (Real et al., 2016; Traore et al., 2017; Traore et al., 2018). Some of these materials with the potential of replacing the NA and which have been widely studied include palm kernel shell, coconut shell, periwinkle shell (Raheem et al., 2008; Regin et al., 2016; Aboshio et al., 2018). The utilization of these materials as aggregate in concrete has been found to be a viable option for their disposal (Bahrami et al., 2015).

PKS is the solid outer covering of palm kernel obtained as a byproduct of oil palm fruit processing. According to FAO (2018), total global oil palm production in 2018 was estimated at 71.45 million tonnes. The world's leading oil palm producing countries are Indonesia, Malaysia, Thailand, Colombia, Nigeria and Guatemala. Nigeria was the world's fifth largest producer of oil palm and Africa's largest, with an estimated output of 1.05 million tonnes in 2018 (FAO, 2018). About 5.5% of the PKS is present in each bunch of fresh fruit from oil palm trees (Teo et al., 2006). PKS is found useful as a source of fuel for cooking, burning and finishes in mud houses (Okpala, 1990). The silicate formed in boilers when it is used as source of fuel has restricted its use in that regards (Poku, 2002). The increase in the studies on the use of PKS is basically to expand the knowledge on the potentials of this materials with the expectation of increasing the extent of its utilization in construction industries. PKS has been found useful as promising aggregate material for reducing the dead weight and thermal conductivity of concrete. For instance, Traore et al. (2017) revealed that the thermal conductivity and diffusivity of concrete decreased by 10% and 42% when coarse aggregate was replaced with 50% PKS; 28% and 42% with full replacement with PKS while the specific heat increased by 56% and 24% at 50% and full replacement of PKS, respectively. Alengaram et al. (2013), discovered that PKS foamed concrete had a thermal conductivity that was 56% lower than conventional bricks. Serri et al. (2014a) reported that PKSC showed lower thermal conductivity than the conventional concrete (CC). Similarly, Traore et al. (2018) found a reduction in thermal conductivity and diffusivity of 28% and 42% by full replacement of NA by untreated PKS; 52% and 33% with polyvinyl alcohol treated PKS while specific heat increased by 24% for untreated PKS and decreased by 29% for the treated PKS. The decrease in thermal conductivity has been attributed mostly to PKS's poor thermal conductivity when compared to that of NA. According to Khan (2002), NA thermal conductivity ranged between 1.16 W/mK and 8.56 W/mK, but PKS thermal conductivity can be as low as 0.45 W/m K (Okpala, 1990).

Mineral admixtures including fly ash, silica fume, corn cob ash, rice husk ash, and saw dust ash have been shown to improve the thermal efficiency of concrete and mortar. The investigation by Demirboğa and Gül (2003) revealed that the thermal conductivity of pumice aggregate concrete with 30% fly ash as substitute for cement reduced by 10% compared with the pumice aggregate concrete without admixture. Demirboğa et al. (2007) indicated that the concrete's thermal conductivity decreased by 23% with the inclusion of 30% fly ash. (Raheem and Adesanya (2011) observed a drop in thermal conductivity of cement mortar with the incorporation of corn cob ash. The study by Raheem et al. (2015) reported a decrease in concrete's thermal conductivity after substituting cement with saw dust ash. Huang et al. (2021) revealed that the thermal conductivity of calcium sulfoaluminate cement-based mortars decreased with increase in the substituting expanded perlite for sand from 0 to 100%.

RHA is obtained from the incineration of rice husk, a major by-product from rice processing industries. According to AMIS (2021), the estimate of commercial harvest of rice globally in 2020/21 was 514.3 million tonnes. Nigeria is Africa's largest rice producer, with an average annual production volume of 8 million metric tons. As of 2019, Nigeria was ranked the 14th largest rice producer in the world, with China being the top producing country (Thrive Agric, 2020). Rice milling produces 200 kg of husk for every ton of rice milled, resulting in 40 kg of RHA after complete combustion (Zerbino et al., 2011). RHA is abundantly available in rice producing countries and the ash obtained from it is rich in silica which make it to be suitable for use as cement replacement material (Nilantha et al., 2010; Soltani et al., 2014; Silva et al., 2020). RHA improves the concrete properties through the filler effect, hydration heat reduction, and the pozzolanic reaction of RHA with cement hydration by-product (Calcium hydroxide) (Jamil et al., 2016; Filho et al., 2017). Several studies (Abalaka, 2013; Raheem and Kareem, 2017; Rattanachu et al., 2020), have shown that the inclusion of RHA as substitute for cement enhanced the compressive strength of concrete and mortar. Amorphous RHA exhibited high resistance to chemical corrosion and temperature variation, low thermal conductivity, high melting point, low bulk density and high porosity (Silva et al., 2020; Chindaprasirt et al., 2007; Bahrami et al., 2016; Praveenkumar et al., 2019). In recent studies (Raheem and Kareem, 2017; Rattanachu et al., 2020), RHA was incorporated into PKSC. Foong et al. (2015) compared the strength properties of RHA based PKSC and PKSC without RHA. Philips et al. (2017) also related the strength and water absorption characteristics of RHA based PKSC and NA.

Because of RHA's advantages as a mineral admixture, its combination with PKS is bound to enhance PKSC qualities. The modification of PKSC with RHA leads to further reduction of PKSC density resulting to further reduction of thermal conductivity of PKSC as a lightweight concrete. As a result, the use of these materials would aid the construction of structural concrete with a lower dead load than CC with the benefit of cost saving and ease of construction. The extra calcium-silicate-hydrate (C-S-H) gel produced in concrete as a result of the RHA pozzolanic activity during the cement hydration refines the concrete pores and improves the interfacial transaction zone in between aggregates and cement paste, resulting in a denser internal structure in concrete. As a result, the strength of concrete is expected to rise (Soltani et al., 2014). A large quantity of PKS or RHA are usually stockpiled and subsequently dump as residue thereby constituting a nuisance and environmental pollution especially in an area where they have been accumulated in large quantities. Thus, the use of these materials as construction purposes is considered as the environmental-friendly method of their disposal (Raheem and Kareem, 2017). In addition, utilization of these materials will encourage increase in rice and oil palm productions. The increase in production will substantially increase farmer wages, provide economic incentive for the community, and contribute to the country's gross domestic product.

Based on the literature, the strength characteristics of PKSC with RHA as mineral admixture were studied at an early age of up to 28 days. Furthermore, there is paucity of research on the thermal properties of PKSC blended with RHA. Therefore, this study investigates the oven-

Table 1
Chemical compositions of cement and RHA.

Materials	Chemical composition (%)										
	SiO_2	Al_2O_3	Fe_2O_3	CaO	MgO	SO_3	K_2O	Na_2O	Others	$SiO_2 + Al_2O_3 + Fe_2O_3$	*LOI
Cement	20.92	4.84	3.24	62.50	2.53	2.77	0.19	0.25	2.76	29	1.52
RHA	92.40	0.78	1.06	1.38	1.09	0.06	1.63	0.04	1.56	94.24	8.93

* LOI = Loss On Ignition.

Table 2
Physical properties of Aggregates.

Properties	Materials		
	River sand	Granite	PKS
Maximum size (mm)	2.36	20	20
Fineness Modulus	2.52	2.59	2.37
Specific gravity	2.79	2.91	1.19
Water absorption (%)	15.03	7.93	16.99
Bulk density (kg/m^3)	1802	1614	762

dry bulk density, compressive strength, and thermal properties (thermal conductivity, thermal diffusivity, volumetric heat capacity, and thermal resistivity) of concrete of three different mix proportions produced with PVA-treated PKS as a substitute for NA and RHA as a partial substitute for cement.at the curing ages of up to 90 days. The findings from this study would be useful in establishing mix proportioning and understanding the behavior of RHA-blended PKSC.

2. Materials and method

2.1. Materials

Portland limestone cement, river sand, crushed granite, PKS, rice husk, polyvinyl alcohol (PVA) and water are the materials used in this study. Elephant brand of cement of grade 32.5 N with the specific gravity of 3.19 which conformed to BS EN 197-1 (2011) was used as binder in the concrete mix. River sand of 4.75 mm maximum size sourced from the river bank along Ifon Osun, Osun State Nigeria was the fine aggregate used. Crushed granite was sourced from the Quarry site at Ibadan. PKS of 20 mm nominal size was collected from mini oil palm processing mill at Ogbaagba community, Osun State, Nigeria. The collected PKSs were first washed with detergent soap and subsequently dipped in portable water and 5% PVA solution for up to 24 ± 2 *h* in line with Thong et al. (2017). Previous studies (Traore et al., 2018; Thong et al., 2017) have established that this treatment method is effective in improving the quality of PKS in terms of water absorption. RH was sourced from mini rice processing mill within Ogbomoso, Oyo State, Nigeria.

RHA was produced by calcinating the husks in the furnace at the temperature of 600 ^{O}C for 4 h. The chemical compositions of cement and RHA are presented in Table 1. The RHA was subsequently sieved with 75 μm sieve to obtain the ash having the specific gravity and bulk density values of 1.90 and 145 kg/m^3, respectively. Fig. 1(a)-(d) show the granite, river sand, PKS and RHA samples used in the analysis, respectively. The particle-size distribution and the properties of aggregates are shown in Fig. 2 and Table 2, respectively. RHA had SiO_2 (92.40%) as its major chemical constituent. The SO_3 of RHA does not exceed the maximum of 5% specified by (ASTM C618–12 (2012) for cementitious material. These validate the previous findings (Raheem and Kareem, 2017; Rattanachu et al., 2020; Nguyen, 2021). The sum of SiO_2, Al_2O_3 and F_2O_3 for RHA was 94.24% that is more than 70% and LOI of 4.64 which is less than 6% as specified by ASTM C618–12 (2012) for class F pozzolans. The potable water collected from the tap at the Structural and Material Laboratory at Civil Engineering Laboratory, Ladoke Akintola University, Ogbomoso, Nigeria was used throughout the experimental works.

2.2. Mix design, batching and sampling

Three control concrete mixes with prescribed mix ratios of 1:1$\frac{1}{2}$:3, 1:2:4 and 1:3:6 using water-to-cement (w/c) ratios of with w/c ratio of 0.5, 0.6 and 0.7, respectively were made with cement, river sand and granite. For each mix ratio with the respective w/c ratio, five concrete mixes containing RHA fixed at 15% as replacement for cement and PKS at the rate of 20, 40, 60, 80 and 100% as replacement for crushed granite by volume were produced. The sample prepared without PKS and served as the control. The PKS which was in saturated surface dry condition was used during aggregate mixing. The cement used for concrete mixes was replaced with a fixed amount of 15% of RHA except the control. Concrete mixing was done manually according to BS 1881-125 (2013) Concrete mixes were then cast into wooden moulds and placed in the curing room at 27 ± 5 ^{O}C. After 24 h, the concrete specimens were unmoulded and later cured in water until the testing ages.

2.3. Testing methods

2.3.1. Density

The density of hardened concrete specimens was determined at 28 days of curing in accordance with ASTM C642-13 (2013).

2.3.2. Compressive strength

Concrete specimens' compressive strength was determined in accordance with ASTM C39/C39M-12 (2012). Concrete specimens measuring $100 \times 100 \times 100$ mm were cast in steel moulds in three layers and manually compacted with 25 strokes of a steel tamping rod with a diameter of 25 mm across the cross section of the mold. The specimens were demoulded after 24 h and water cured in a curing chamber for 7, 28, 56, and 90 days before being tested. On each testing age, three specimens from the same concrete mixture were removed from the curing tank and allowed to dry at room temperature for two hours before being crushed on a compression machine (maximum capacity 2000 kN). The compressive strength was based on the average of three specimens.

2.3.3. Thermal properties measurement

The thermal properties (thermal conductivity, thermal diffusivity, volumetric heat capacity and thermal resistivity) of concrete specimens were determined using a direct measuring instrument with surface probe known as KD2 Pro-thermal properties analyzer by Decagon Inc. devices Fig. 3). This instrument measured the thermal properties of materials based on transient heat source methods as specified in ASTM D5334–14 (2014). The transient methods measures the thermal properties within several minutes as a result of its ability to record temperature signal during a heating process (Huang et al., 2021). A needle with an internal heater and temperature sensor was used as a probe for this measurement. A current is passed through the heater, and the system continuously monitors the sensor's temperature over time. The thermal conductivity of a sensor is determined by analyzing its temperature. According to Carslaw and Jaeger (1959) and Kluitenberg et al. (1993), the KD2 Pro employs two distinct algorithms, one for the dual needle sensor and one for the single needle sensor. For the Dual needle algorithm, heat is applied to the heated needle for a given heating time, th, and temperature is measured in the monitoring needle, 6 mm distance, during the cooling period following heating. The reading can be processed by removing

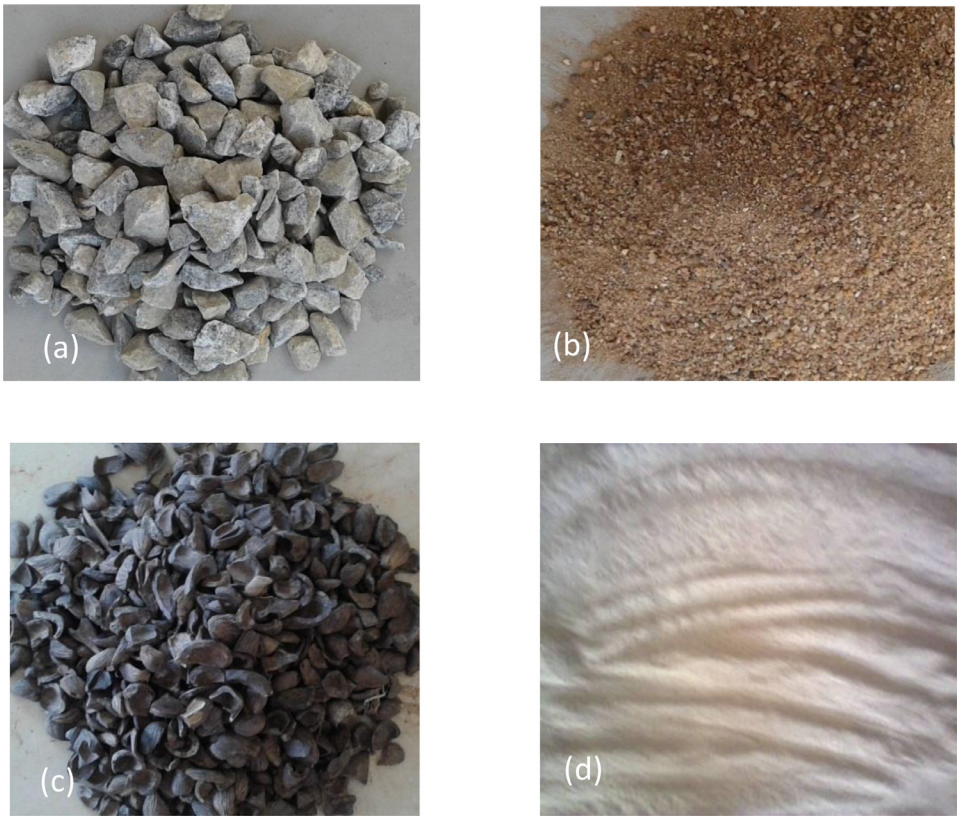


Fig. 1. (a) Granite sample; (b) River Sand sample; (c) PKS sample; and (d) RHA sample.

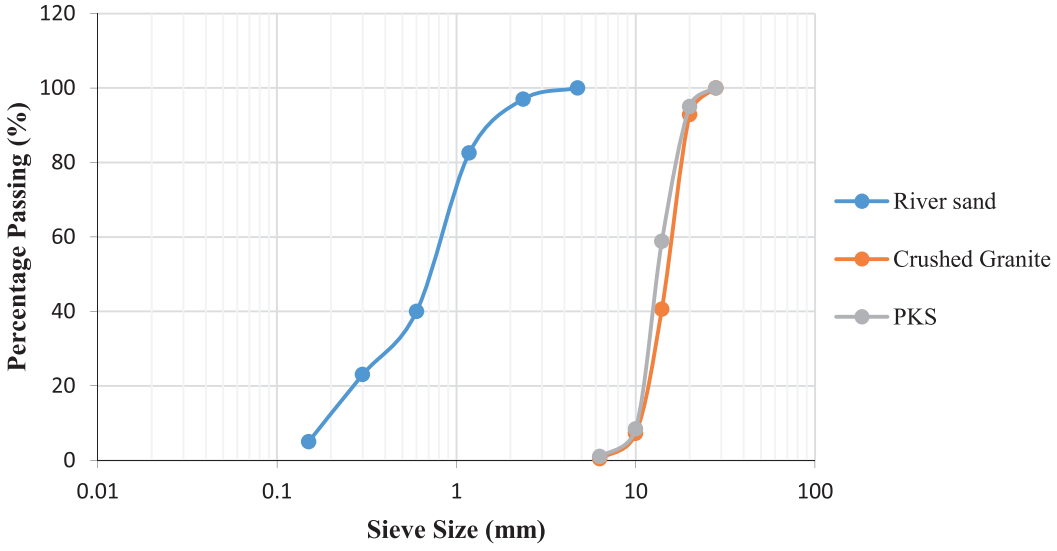


Fig. 2. Gradation curves of aggregates.

the ambient temperature at time 0, multiplying by 4, and dividing by the heat per unit length, q. Using a non-linear least squares approach, the obtained data is fitted to the following equations as demonstrated by Eq. (1). Eqs. (1) and ((2) apply to the first th seconds when the heat is turned on and off, respectively. Thermal conductivity and diffusivity can be calculated using Eqs. (4) and (5). Eqs. (6) and (7) can be used to calculate volumetric specific heat and thermal resistance (7).

$$T^* = b_0 t + b_1 Ei\left(\frac{b_2}{t}\right) \tag{1}$$

$$T^* = b_0 t + b_1 \left\{ Ei\left(\frac{b_2}{t}\right) - Ei\left[\frac{b_2}{t - t_h}\right] \right\} \tag{2}$$

$$T^* = \frac{4\pi\left(T - T_0\right)}{q} \tag{3}$$

$$k = \frac{1}{b_1} \tag{4}$$

$$D = \frac{r^2}{4b_2} \tag{5}$$

$$C_v = \rho C_P = \frac{K}{4b_2} \tag{6}$$

$$r = \frac{1}{K} \tag{7}$$

Where: *Ei* is the exponential integral, b_0, b_1 and b_2 are the constants to be fit. T_0 is the temperature at the start of the measurement and q is



Fig. 3. Setup for thermal properties test.

the heat input, K is the thermal conductivity, D is the diffusivity, C_v is the volumetric heat capacity, C_p is the specific heat capacity, ρ is the density and r is the thermal resistivity.

In this study, Pilot pins of 1.3 mm diameter x 30 cm long, 6 mm spacing coated with Vaseline were installed from the surface of the specimens while in fresh state to create the hole that will accommodate the sensor probe of thermal analyzer. The pins were removed when the concrete specimens have hardened. The surface probe/sensor used is a 30 cm dual-needle (SH-1). The sensor was coated with thermal grease and embedded into the cast hole on the specimen surface to take the readings. Three specimens from the same concrete mixture were taken out of the curing compartment after being cured for 7, 28, 56 and 90 days and oven-dried at 100 to 115 ^{o}C using the electric drying oven, until a constant mass was reached to remove the moisture in line with the literatures (Sengul et al., 2011; Traore et al., 2017). The specimens were left to settle to ambient temperature before taking thermal properties readings from the thermal analyzer's display unit after inserting the sensor from the device into the hole formed on the specimen earlier while it was still fresh, as illustrated in Fig. 3. The value for each of the thermal characteristics was calculated using the average of three specimens.

3. Results and discussion

3.1. Density

Fig. 4 presents the results of 28-day density of RHA-blended PKSC with different mix ratios. It can be noted from Fig. 4 that the percentage of PKS present in concrete and the mix ratios had significant effect on oven-dry bulk density of concrete. For 1:1$^{1}/_{2}$:3 mix ratio, the average oven-dry density decreased from 2431 to 1600 kg/m^3 with increased in PKS replacement at 0–100%; while for 1:2:4 mix ratio, the density decreased from 2256 to 1404 kg/m^3 with increase in PKS contents from 0 to 100% and the average oven-dry density values of concrete produced with 1:3:6 mix ratio decreased from 2104 to 1256 kg/m^3 as the PKS contents increased from 0 to 100%. These findings are in consistent with previous researches (Alengaram et al., 2013; Philips et al., 2017; Sobuz et al., 2014; Maghfouri et al., 2018), where the concrete density declined as the content of PKS aggregate increased. The lower bulk density of PKS, which is approximately 58% lower than that of granite (Table 1) may account for the reduction in concrete density. Therefore, the substitution of granite with PKS in CC increased the void content which subsequently reduced the concrete density. The RHA included in concrete is also beneficial for the reduction in concrete density since it exhibited lower specific gravity (1.94) than cement (3.19) (Praveenkumar et al., 2019; Damdelen et al., 2014). Concrete with an oven-dry density of less than 2000 kg/m^3 is classified as structural LWA concrete (LWAC) by Newman and Owen (2003). This density range was observed at the substitution levels of granite with PKS of 60% and above for mix ratio 1:1$\frac{1}{2}$:3, 40% and above for mix ratio 1:2:4 and 20% and above for mix ratio 1:3:6. The maximum reductions of

31%, 34% and 38% in the density of concrete were observed for concrete with 1:1$\frac{1}{2}$:3, 1:2:4 and 1:3:4 mix ratios, respectively, at 100% PKS and 15% RHA combination at 90-day curing age with respect to the control for mix ratio.

As shown in Fig. 4, the density of RHA-blended PKSC is altered by the aggregate/cement ratio of concrete mix. The concrete specimens produced with the richer concrete mix (1:1$\frac{1}{2}$:3), having lower aggregate/cement ratio exhibited higher density values than those with 1:2:4 mix ratio while the values with 1:2:4 mix ratio were also higher than those with 1:3:6 mix ratio. As the aggregate content increased, the void content of the concrete mix is expected to rise while its level of compactness decreased. Thus, the density of concrete with higher aggregate content is lower than that with lower aggregate content. This corroborates previous findings regarding concrete or mortar produced with different mix ratios (Okpala, 1990; Sobuz et al., 2014; Olanipekun et al., 2006; Braga et al., 2014; Kareem et al., 2021). It can be deduced that the reduction of concrete oven-dry density means that the combination of both materials (PKS and RHA) is ideal for use as lightweight and green concrete. Such concrete has the tendency of exhibiting lower self-weight thereby resulting to reduction in load on foundation and building structures with the benefit of cost saving and ease of construction. In addition, better thermal properties that guarantee better thermal comfort for human and animals.

3.2. Compressive strength

The compressive strength of RHA-blended PKSC with various mix ratios at curing ages of 7, 28, 56 and 90 days are shown in Fig. 5. For all the mix ratios examined, the compressive strength improved with increasing curing ages and declined with increasing PKS substitution. At 7 days, the compressive strength values control were 20.83 N/mm^2, 17.63 N/mm^2 and 14.67 N/mm^2 for 1:1$\frac{1}{2}$:3, 1:2:4 and 1:3:6 mix ratios, respectively. The substitution rate of PKS has a substantial influence on the compressive strength of concrete with the addition of PKS. For example, when the PKS substitution rate increased from 20% to 100%, the 7-day compressive strength of RHA-blended PKSC for a 1:1$\frac{1}{2}$:3 mix ratio decreased from 17.17 to 9.97 N/mm^2. This trend is similar to the compressive strength of RHA-blended PKSC at various ages for varied mix ratios. These findings are consistent with earlier research (Traore et al., 2017; Philips et al., 2017; Sobuz et al., 2014; Maghfouri et al., 2018; Djima et al., 2018; Azunna, 2019). As illustrated in Fig. 5, incorporating PKS remarkably increased the concrete void contents and reduced its density. Consequently, the compressive strength of concrete declined. Furthermore, the increased surface area, fineness, and flakiness of PKS reduced concrete workability and resulted in a weakening of the bond between the aggregate and the hydrating cement paste, resulting in lower compressive strength (Okpala, 1990; Maghfouri et al., 2018; Osei and Jackson, 2012). However, it was noted that up to 60–70% of the 28-day strength was attained at 7 days by RHA-blended PKSC for mix ratios. For instant, about 87% to 85%, 86% to 87% and 86 to 83% of 28-day strength were achieved by RHA-blended PKSC when PKS replacement ratio increased from 20% to 100% for 1:1$\frac{1}{2}$:3, 1:2:4 and 1:3:6 mix ratios, respectively. The early strength developed by RHA-blended PKSC can be ascribed to the filler action of RHA, which decreased the porosity of concrete, and this was proposed to be advantageous in precast concrete where early strength is critical (Foong et al., 2015).

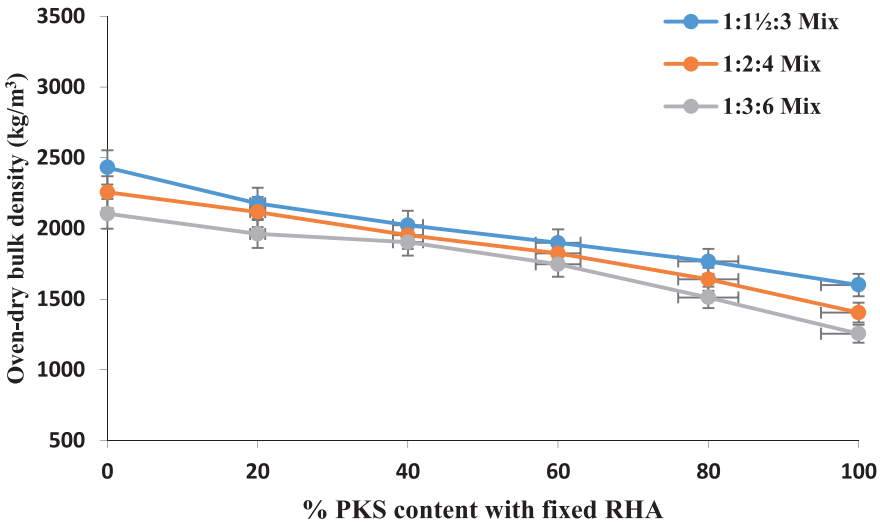


Fig. 4. Oven-dry bulk density of RHA-blended PKSC at 28 days.

In addition to PKS substitution rate, the compressive strength of RHA-blended PKSC is also affected by the curing ages as revealed in Fig. 5. For example, from 7 days to 90 days, the compressive strength increased about 7.9–8.3 N/mm^2, 5.6–6.9 N/mm^2, 6.2–8.0 N/mm^2, 6.6–7.2 N/mm^2, 5.6–6.2 N/mm^2, 4.0–5.8 N/mm^2, for RHA-blended PKSC at 0%, 20%, 40%, 60%, 80% and 100% PKS substitution, respectively. This corroborates previous studies (Maghfouri et al., 2018; Olanipekun et al., 2006; Shafigh et al., 2012), where the concrete strength improved as the curing ages increased. As the curing age increases, the voids between the concrete particles (cement grains and aggregate) are filled by additional hydration products produced, thereby increasing the concrete density. Consequently, the concrete's strength increases (Okpala, 1990; Ulykbanov et al., 2019; Uysal et al., 2004).

The compressive strength of RHA-blended PKSC was also found to be influenced by the aggregate/cement ratio of the concrete mix. For example, the compressive strength of control (without PKS and RHA) with 1:3:6 mix ratio having the highest aggregate/cement ratio was 2.5 N/mm^2 and 6.0 N/mm^2 lower than those with 1:1$\frac{1}{2}$:3 and 1:2:4 mix ratios, respectively. This can be attributed to the fact that when the aggregate/cement ratio increased, as in the instance of 1:3:6, the amount of cement available was insufficient to adequately bond with the aggregate, resulting in a loss in the compressive strength of RHA-blended PKSC. However, for the richest concrete mix (1:1$\frac{1}{2}$:3) with lower aggregate/cement ratio, the void contents of the concrete decreased as the aggregate content decreased, while the level of compactness improves. As a result, fine cement particles fill up the spaces in the aggregate, improving the physical packing of the aggregate and producing more C-S-H, which enhances the compressive strength of concrete (Braga et al., 2014; Kareem et al., 2021).

It was also noted from the results that the inclusion of RHA had influence on compressive strength of RHA-blended PKSC as the greater strength gain were observed for RHA-blended PKSC than the control as curing age increased from 28 days to 90 days. For example, The gain in compressive strength from 28 to 90 days for control was 7%, 13%, and 16% for control with 1:1$\frac{1}{2}$:3, 1:2:4, and 1:3:6 mix ratios, respectively, while it ranged from 18 to 24%, 15–23%, and 18–27% for RHA-blended PKSC with the respective mix ratios. The pozzolanic action of concrete containing RHA was proven by the increase in the strength development of RHA-blended PKSC. Chao-Lung et al. (2011) achieved comparable results in CC utilizing RHA as a substitute for cement. This suggests that as the curing progresses, the rate of strength development will accelerate. The increase in strength gain observed for RHA-blended PKSC compared to those without RHA was related to the extra C-S-H gel formed due to the pozzolanic action of RHA, which enhanced particle packing and hence improved the microstructure of PKSC.

The presented results, as shown in Fig. 5, indicated that the control achieved the minimum NWC strengths of M25 for a 1:1$\frac{1}{2}$:3 mix ratio, M20 for a 1:2:4 mix ratio, and M15 for a 1:3:6 mix ratio at the curing age of 28 days, as stipulated in BS EN 1992–1–1:2004 + A1 2014 (2014). All the RHA-blended PKSC exhibited the compressive strength below the targeted strength for NWC for the respective mix ratio investigated. However, the RHA-blended PKSC containing 20% PKS showed slight reduction compared with the targeted values while those containing higher PKS content showed higher reduction for the respective mix ratio. In addition, the compressive strength value of 17 N/mm^2 specified by ASTM C 330/C 330 M (2014) and -ACI 213R-03 (2003) for Structural LWAC at the curing age of 28 days was satisfied by RHA-blended PKSC containing PKS content up to 40% for 1:1$\frac{1}{2}$:3 mix ratio, 20% for 1:2:4 mix ratio, while for 1:3:6 mix ratio, all the PKS replacement considered could not satisfy ASTM C 330/C 330 M (2014) ASTM C 330/C 330 M (2014) and ACI 213R-03 (2003) requirements.

The scatter plot showing the correlation between concrete 28-compressive strength and oven-dry density of RHA-blended PKSC is shown in Fig. 6. The compressive strength of RHA-blended PKSC and the oven-dry density decreased linearly as the aggregate replacement ratio with PKS increased with the coefficient of determination (R^2 = 0.988). Maghfouri et al. (2018) and Liu et al. (2014) provided similar relationship for oil palm shell foamed geopolymer concrete and PKSC, respectively.

3.3. Thermal conductivity

Fig. 7 shows the outcomes of RHA-blended PKSC with varied mix ratios at curing ages of 7, 28, 56, and 90 days. The thermal conductivity of RHA-blended PKSC was significantly affected by the PKS substitution rate. For 1:1$\frac{1}{2}$:3 mix ratios, at 28 days, thermal conductivity of RHA-blended PKSC decreased from 1.61 W/mk to 1.30 W/mk, 0.86 W/mk, 0.67 W/mk, 0.63 W/mk and 0.51 W/mk when the PKS contents increased from 0%, 20%, 40%, 60%, 80% and 100%, respectively. A comparable trend was found for RHA-blended PKSC with other mix ratios for different ages. These agree with previous studies (Traore et al., 2017; Alengaram et al., 2013; Serri et al., 2014b), where the concrete thermal conductivity of declined as the PKS contents increased. The lower thermal conductivity of RHA-blended PKSC is caused by the insulating effect of PKS, which has a lower thermal conductivity than NA (Traore et al., 2017; Alengaram et al., 2013). The thermal conductivity of PKS can be as low as

0.45 W/mK (Bahrami et al., 2015), while the thermal conductivity of NA varied between 1.16–8.56 W/mK (Khan, 2002). The in-

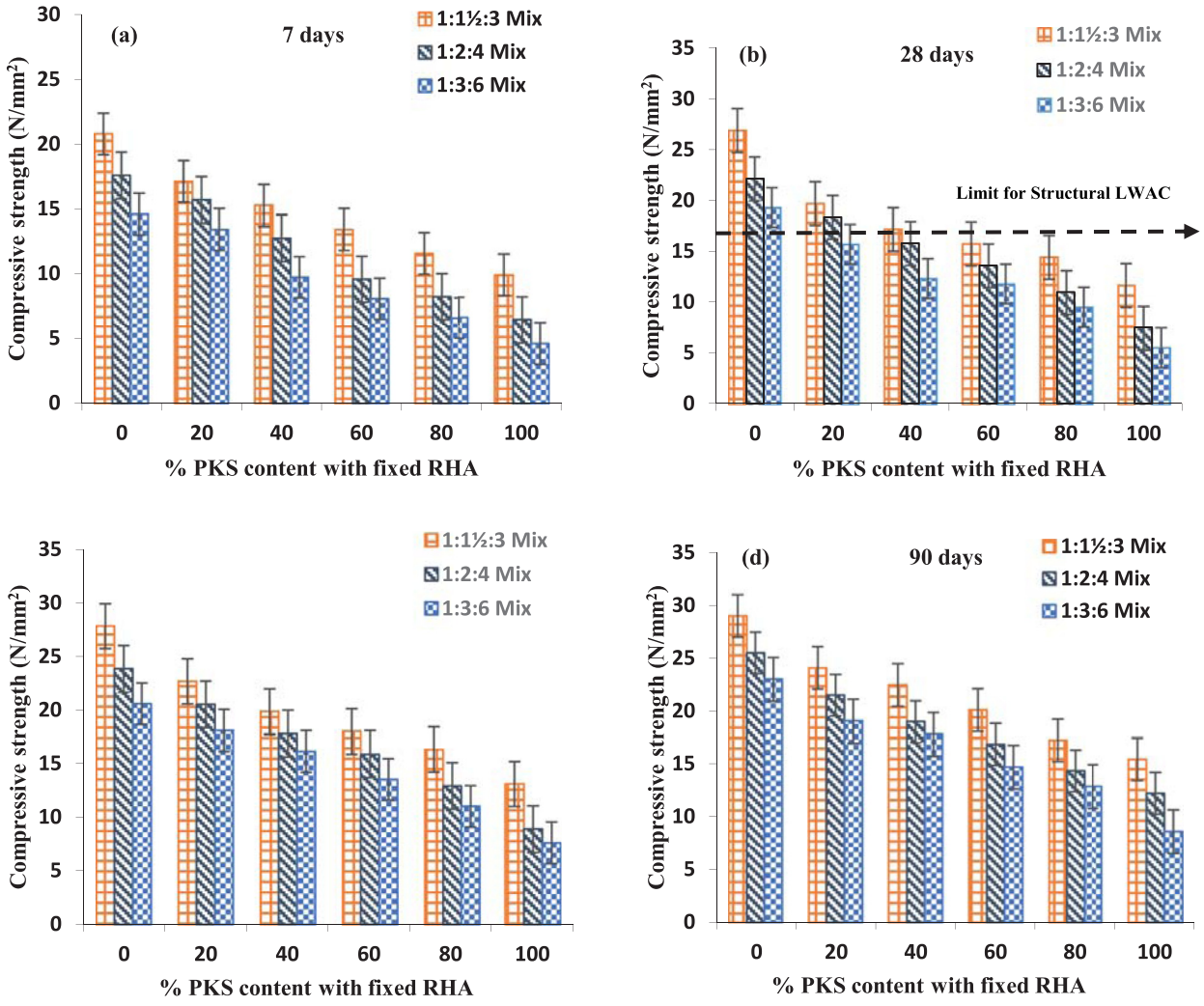


Fig. 5. Compressive strength of RHA-blended PKSC at: (a) 7 days; (b) 28 days; (c) 56 days; and (d) 90 days.

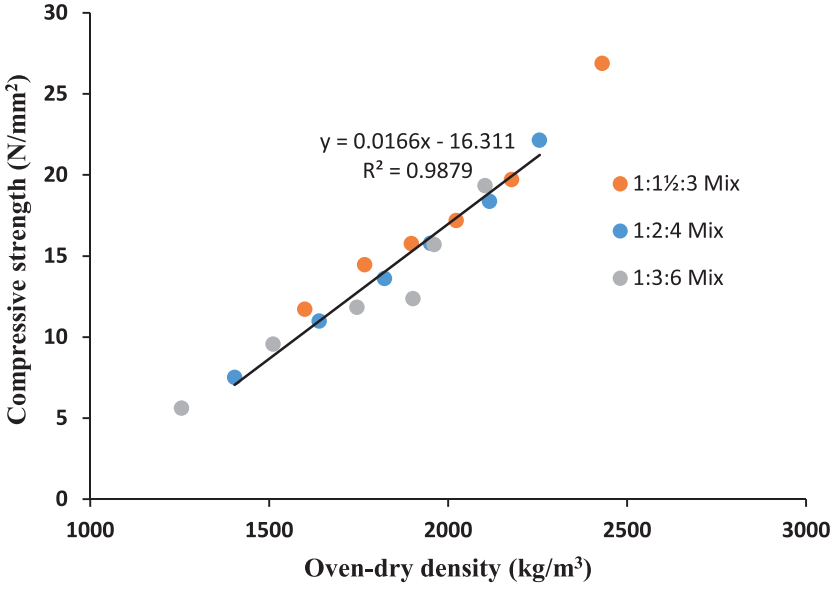


Fig. 6. Correlation between Oven-dry density and compressive strength.

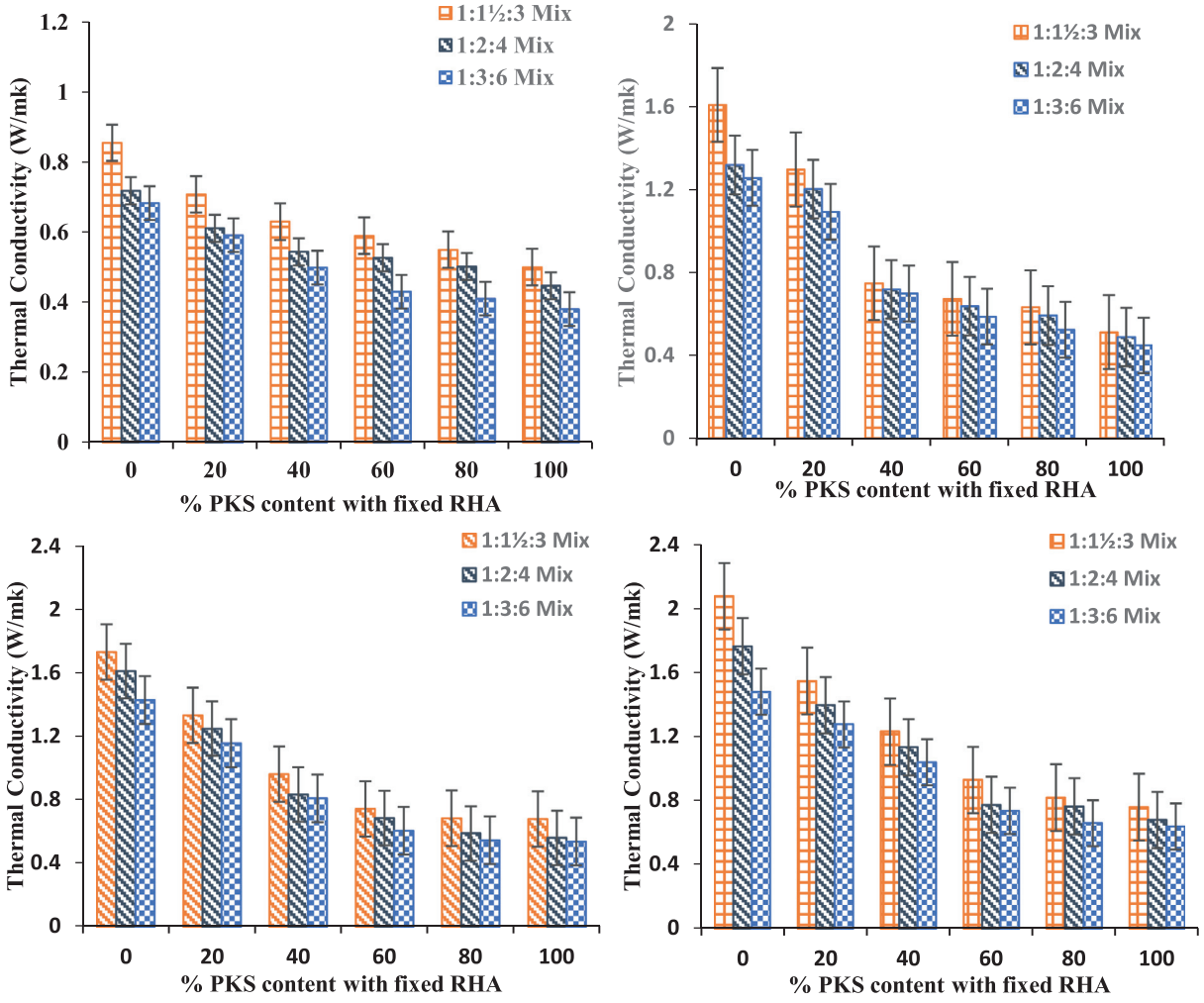


Fig. 7. Thermal conductivity of RHA-blended PKSC at: (a) 7 days; (b) 28 days; (c) 56 days; and (d) 90 days.

crease in void content leading to the reduction in concrete density due higher porosity PKS compared to NA is also responsible for the decrease thermal conductivity of RHA-blended PKSC (Traore et al., 2017; Okpala, 1990; Alengaram et al., 2013; Serri et al., 2014b). Since RHA has a lower specific gravity and a higher active silica content than cement, it can also contribute to the fall in thermal conductivity in concrete (Praveenkumar et al., 2019; Damdelen et al., 2014). The findings from the present study demonstrates that incorporating PKS and RHA into concrete had a beneficial impact on its thermal and insulation capabilities. Thus, buildings energy consumption and the aftereffect of greenhouse gas emissions are expected to drastically reduce with the use of these materials in buildings. Furthermore, PKS in concrete can effectively reduce the indoor temperature in a building due to low heat conduction from the outside in a hot weather setting, and this effect is amplified when RHA is present. This concrete form may also be useful in the construction of storage structures that involve materials with low thermal conductivity.

The thermal conductivity of RHA-blended PKSC is also affected by curing age as shown in Fig. 7. The thermal conductivity decreased approximately 1.22–0.8 W/mK, 0.84–0.69 W/mK, 0.6–0.54 W/mK, 0.34–0.25 W/mK, 0.27–0.25 W/mK, 0.26–0.23 W/mK, for RHA-blended PKSC at 0%, 20%, 40%, 60%, 80% and 100% PKS substitution, respectively as the curing age rise from 7 days to 90 days. The increase in thermal conductivity with curing age can be ascribed to the fact that the voids between the concrete particles (cement grains and aggregate) are filled by extra hydration products produced, thereby increasing the concrete density. Consequently, the concrete's thermal conductivity increases (Ulykbanov et al., 2019; Uysal et al., 2004). Raheem et al. (2015) provided similar results where the thermal conductivity values improved as curing age increased for concrete with saw dust ash as partial cement substitute. Kim et al. (2003) discovered that curing age had no effect on thermal conductivity of Ordinary Portland Cement (OPC)-based concrete, except for the first two days. Huang et al. (2021) found that curing age had no effect on the thermal conductivity of OPC-based mortars.

The findings also showed that the aggregate/cement ratio of concrete mix had influence on the thermal conductivity of RHA-blended PKSC. For example, the thermal conductivity of control (without PKS and RHA) with 1:3:6 mix ratio having the highest aggregate/cement ratio was 0.6 W/mK and 0.29 W/mK lower than those with 1:1$\frac{1}{2}$:3 and 1:2:4, respectively. These findings are in line with Raheem and Adesanya (2011) which found that the thermal conductivity of OPC-based mortars declined as aggregate/cement ratio increased. Howlader et al. (2012) reported similar where concrete with higher aggregate/cement ratio (1:2:3) exhibited lower thermal conductivity than the richer mix proportion (1:1.5:2) having lower aggregate/cement ratio. These findings may be credited to the fact that incorporation of more aggregate in the mix ratio of 1:3:6 compared to 1:2:4 and 1:1$\frac{1}{2}$:3 mix ratios, resulting in a decrease in cement content of concrete. Serri et al. (2014b) reported that the thermal conductivity of PKSC increased with the rise in cement content. According to Ngohpok et al. (2018) the thermal conductivity of concrete reduced as the filling paste ratio rises, while the porosity of

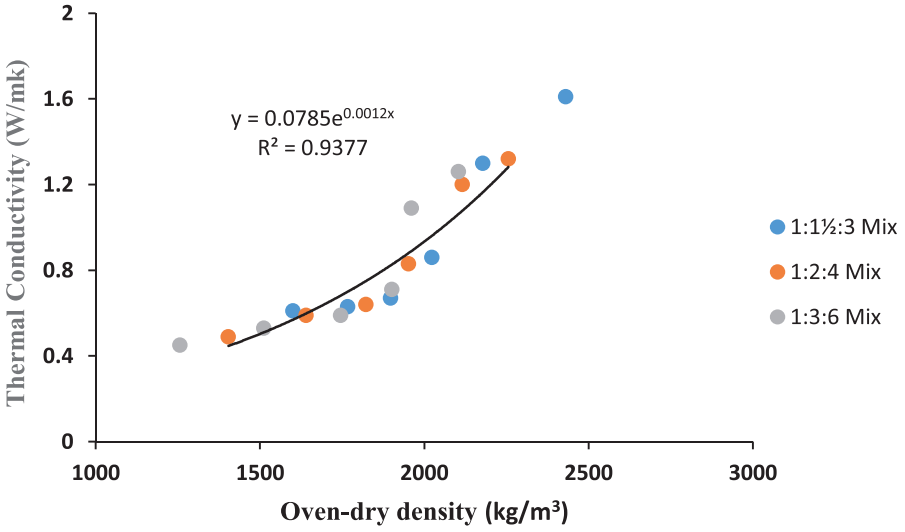


Fig. 8. Correlation between Oven-dry density and compressive strength.

concrete rise with the rise in aggregate content and decline in cement paste.

The results shown in Fig. 7 suggested that the thermal conductivity values for control concrete for the three mix ratios exceeded the value of 1.0 W/mK for LWAC as specified by Newman (1993). All the RHA-blended PKSC containing exhibited the thermal conductivity in the range of 0.2 to 1.0 W/mK for LWAC. The RHA-blended PKSC with PKS addition from 40% PKS and above for all the mix ratios attained the thermal conductivity value below 0.75 W/mK for lightweight concrete useful for insulation purpose. However, the RHA-blended PKSC with PKS addition below 40% PKS exhibited the thermal conductivity value above 0.75 W/mK for lightweight concrete but not useful for insulation purpose according to Newman (1993) and RILEM (1978).

Fig. 8 shows the correlation between the 28-day thermal conductivity and oven-dry density of RHA-blended PKSC. As the inclusion of PKS in the CC increased, the thermal conductivity and oven-dry density of concrete decreased. An exponential correlation with a correlation coefficient (R^2 = 0.938) suggested a very close relationship between the two properties and the prospects of estimating the thermal conductivity from oven-dry density of RHA-blended PKSC. A similar exponential correlation was provided by Huang et al. (2021) for OPC-based mortars. Oktay et al. (2015) also proposed similar correlation to that obtained in Fig. 8 for concrete incorporating different LWAs (pumice, expanded perlite and rubber) as substitute for NA. However, Raheem et al. (2015) proposed a polynomial correlation for corn cob ash blended cement mortar. A polynomial relationships was also proposed by Alengaram et al. (2013) between the thermal conductivity and oven-dry density of oil palm shell foamed concrete.

3.4. Thermal diffusivity

The results of thermal diffusivity of RHA-blended PKSC with various mix ratios at curing ages of 7, 28, 56 and 90 days are presented in Fig. 9. It was noted from the results presented in Fig. 9 that the thermal diffusivity of RHA-blended PKSC followed similar trend as observed for thermal conductivity. The PKS substitution rate caused variation in thermal diffusivity of RHA-blended PKSC. For example, at 28-day, thermal diffusivity of RHA-blended PKSC For 1:1$\frac{1}{2}$:3 mix ratios decreased from 0.60 mm/s^2 to 0.55 mm/s^2, 0.51 mm/s^2, 0.49 mm/s^2, 0.46 mm/s^2 and 0.37 mm/s^2 as the PKS substitution rate increased from 0%, 20%, 40%, 60%, 80% and 100%, respectively. A similar trend was found for RHA-blended PKSC with other mix ratios for different ages. The presented results indicates that the thermal diffusivity of RHA-blended PKSC is affected by the substitution of PKS for granite as it's decreased as the PKS substitution increased. These results confirmed the observations from previous studies (Traore et al., 2017; Serri et al., 2014b; Zulkarnain et al., 2014), where the thermal diffusivity of PKSC as the PKS contents increased. These results also agree with the findings of Oktay et al. (2015) for other LWAs where increase in the contents of pumice, expanded perlite and rubber as substitute for NA resulted to increase in the thermal diffusivity of concrete. The reduction in thermal diffusivity of RHA-blended PKSC can be attributed to the fact that the addition of PKS and RHA increased the concrete void content due to their higher porosity, thereby lowering the concrete density and subsequently the thermal diffusivity of concrete. The lower density of concrete is due to its higher porosity and can also be related to the specific gravity of the lightweight materials (PKS) (Serri et al., 2014a; Serri et al., 2014b; Tandiroglu, 2010). The lower specific gravity and higher active silica content of RHA also contributed to the reduction in thermal diffusivity of concrete compared with cement (Praveenkumar et al., 2019; Damdelen et al., 2014; Hossain et al., 2017). Because RHA-blended PKSC has a lower thermal diffusivity, the temperature differential between indoor and outdoor will take longer to reach equilibrium than in CC (Huang et al., 2021). Concrete with low thermal diffusivity reacts slowly to temperature differences and are effective thermal mass elements in a building accordance to ACI 122R-14 (2014). This concrete type could also act as a heat sink/source to buffer temperature extremes that occur during the diurnal cycle, implying that it has a propensity to lower indoor temperatures when compared to structures made of traditional concrete (Bentz et al., 2011).

The results also revealed that the thermal diffusivity of RHA-blended PKSC is also influenced by the curing age as shown in Fig. 9. For example, the thermal diffusivity decreased about 0.24–0.19 mm/s^2, 0.20–0.19 mm/s^2, 0.21–0.19 mm/s^2, 0.23–0.21 mm/s^2, 0.21–0.19 mm/s^2, 0.19–0.16 mm/s^2, for RHA-blended PKSC with 0%, 20%, 40%, 60%, 80% and 100% aggregate replacement ratio, respectively as the curing age increased from 7 days to 90 days. The increase in thermal diffusivity with curing age can be attributed to the fact that the additional hydration products are produced with increase in curing age thereby filling the concrete's voids (Ulykbanov et al., 2019). As a result, the concrete density rises while the thermal diffusivity decreases. Raheem et al. (2015) found that the thermal diffusivity of concrete using saw dust ash as a partial cement substitution increased with curing age. Hansen et al. (1982) found that the thermal diffusivity of cement paste decreased with curing age. According to Huang et al. (2021) curing age had no effect on the thermal diffusivity of OPC-based mortars.

The presented results in Fig. 9 showed that the aggregate/cement ratio of concrete mix also had influence on the thermal diffusivity of

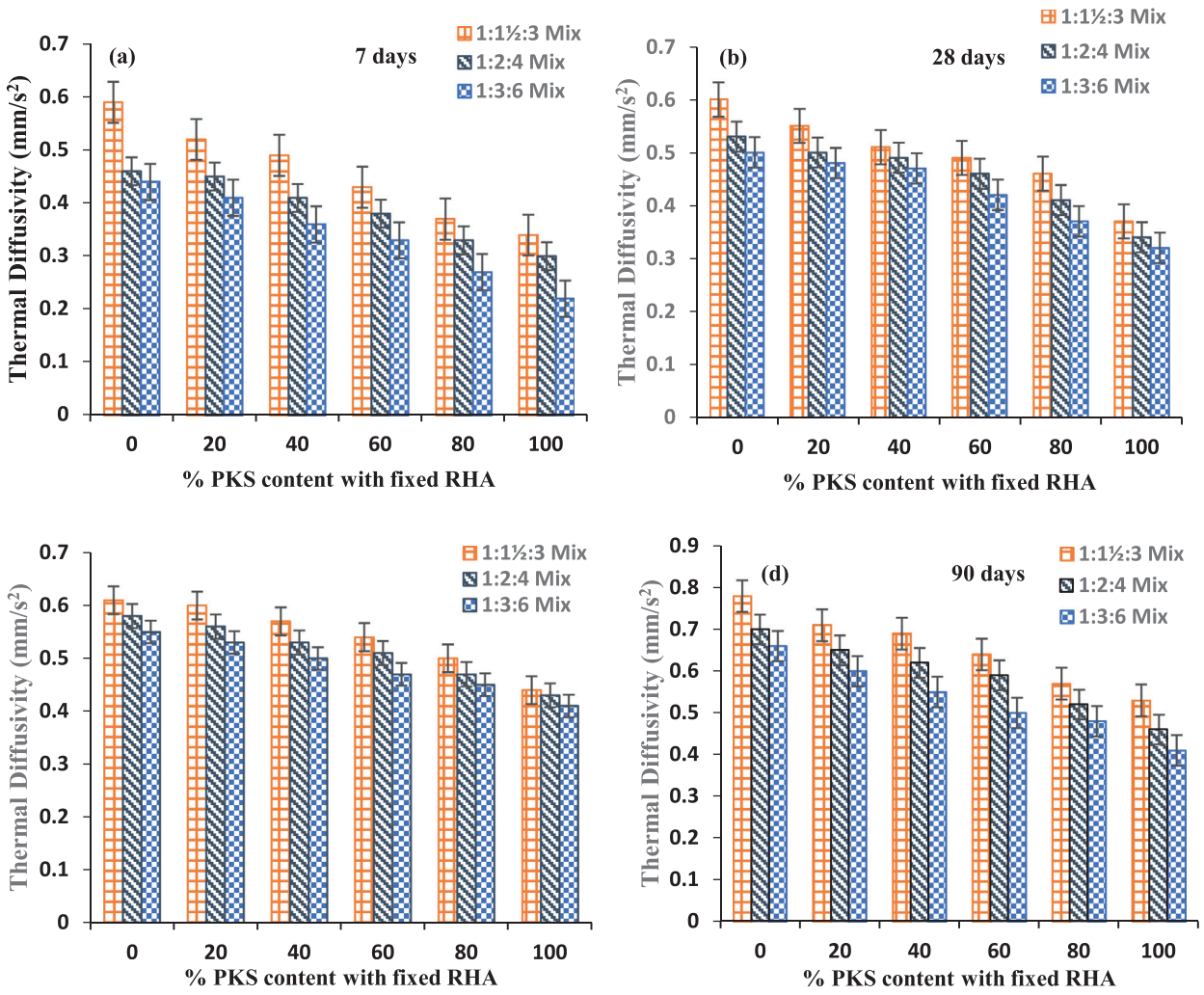


Fig. 9. Thermal diffusivity of RHA-blended PKSC at: (a) 7 days; (b) 28 days; (c) 56 days; and (d) 90 days.

RHA-blended PKSC. For example, the thermal diffusivity of control concrete with 1:3:6 mix ratio having the highest aggregate/cement ratio was 0.15 mm/s^2 and 0.02 mm/s^2 lower than those with 1:1$\frac{1}{2}$:3 and 1:2:4, respectively. These findings agree with Serri et al. (2014b) which found that the thermal diffusivity of PKSC decreased as sand/cement ratio increased. Howlader et al. (2012) reported a similar observation, in which concrete with a richer mix proportion (1:1$\frac{1}{2}$:2) and a lower aggregate/cement ratio exhibited higher thermal diffusivity than concrete with a higher aggregate/cement ratio (1:2:3). The inclusion of more aggregate in concrete mix of 1:3:6 mix ratio compared to 1:2:4 and 1:1$\frac{1}{2}$:3 mix ratios, resulted in a decrease in cement contents, leading to the decrease in concrete density and thermal diffusivity in a similar manner as the thermal conductivity. These can also be ascribed to the rise in the porosity of concrete as the aggregate content rises and the cement paste content decreased.

The 28-day thermal diffusivity values for control concrete were below the ranged of 0.55 and 1.55 mm^2/s as specified Neville (2008) with the exception of the control with 1:1$\frac{1}{2}$:3 mix ratio. However, the thermal diffusivity for all RHA-blended PKSC were below the minimum specified thermal diffusivity value for CC.

The correlation between the 28-day thermal diffusivity and oven-dry density of RHA-blended PKSC is shown in Fig. 10. The thermal diffusivity and oven-dry density of RHA-blended PKSC decreased as the addition of PKS increased, and a correlation with a correlation coefficient (R^2 = 0.941) which show a fair good prediction of thermal diffusivity of RHA-blended PKSC from oven-dry density. A similar correlation was proposed by Oktay et al. (2015) for concrete incorporating other LWAs (pumice, expanded perlite and rubber) as substitute for NA. Huang et al. (2021) also proposed similar correlation for OPC-based mortars.

3.5. Volumetric heat capacity

Fig. 11 presents the results of volumetric heat capacity of RHA-blended PKSC with various mix ratios at curing ages of 7, 28, 56 and 90 days. The results showed that the volumetric heat capacity of RHA-blended PKSC is also influenced by PKS substitution rate. For example, the 28-day volumetric heat capacity increased from 1.39 MJ/m^{3}K to 1.50 MJ/m^{3}K, 1.79 MJ/m^{3}K, 2.13 MJ/m^{3}K, 2.60 MJ/m^{3}K and 3.09 MJ/m^{3}K at from 0%, 20%, 40%, 60%, 80% and

100% PKS replacement, respectively. Similar pattern were observed for RHA-blended PKSC from other mix ratios for different ages. These findings are consistent with the findings of Traore et al. (2017) who discovered that increasing PKS contents from 0% to 100% resulted in an increase in concrete volumetric heat capacity. Oktay et al. (2015) found that increasing the substitution rate of pumice, expanded perlite, and rubber as substitutes for NA increased the volumetric heat capacity of concrete. The increase in volumetric heat capacity can be related to the increase in void content and a reduction in concrete density with aggregate (PKS) with a higher porosity than the NA. The presence of high SiO_2 and low Al_2O_3 in RHA, as well as its lower specific gravity compared to cement, may contribute to the high specific heat capacity of incorporating PKS and RHA (Praveenkumar et al., 2019; Kareem et al.,

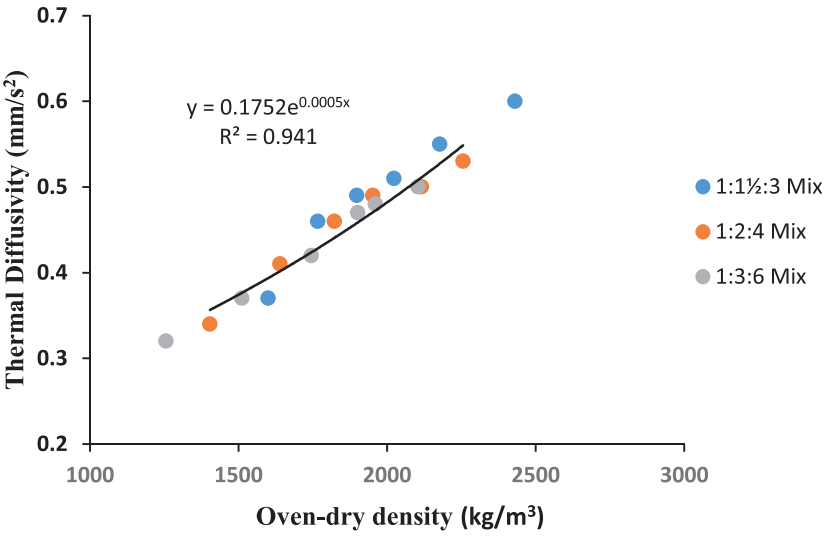


Fig. 10. Correlation between Oven-dry density and thermal diffusivity.

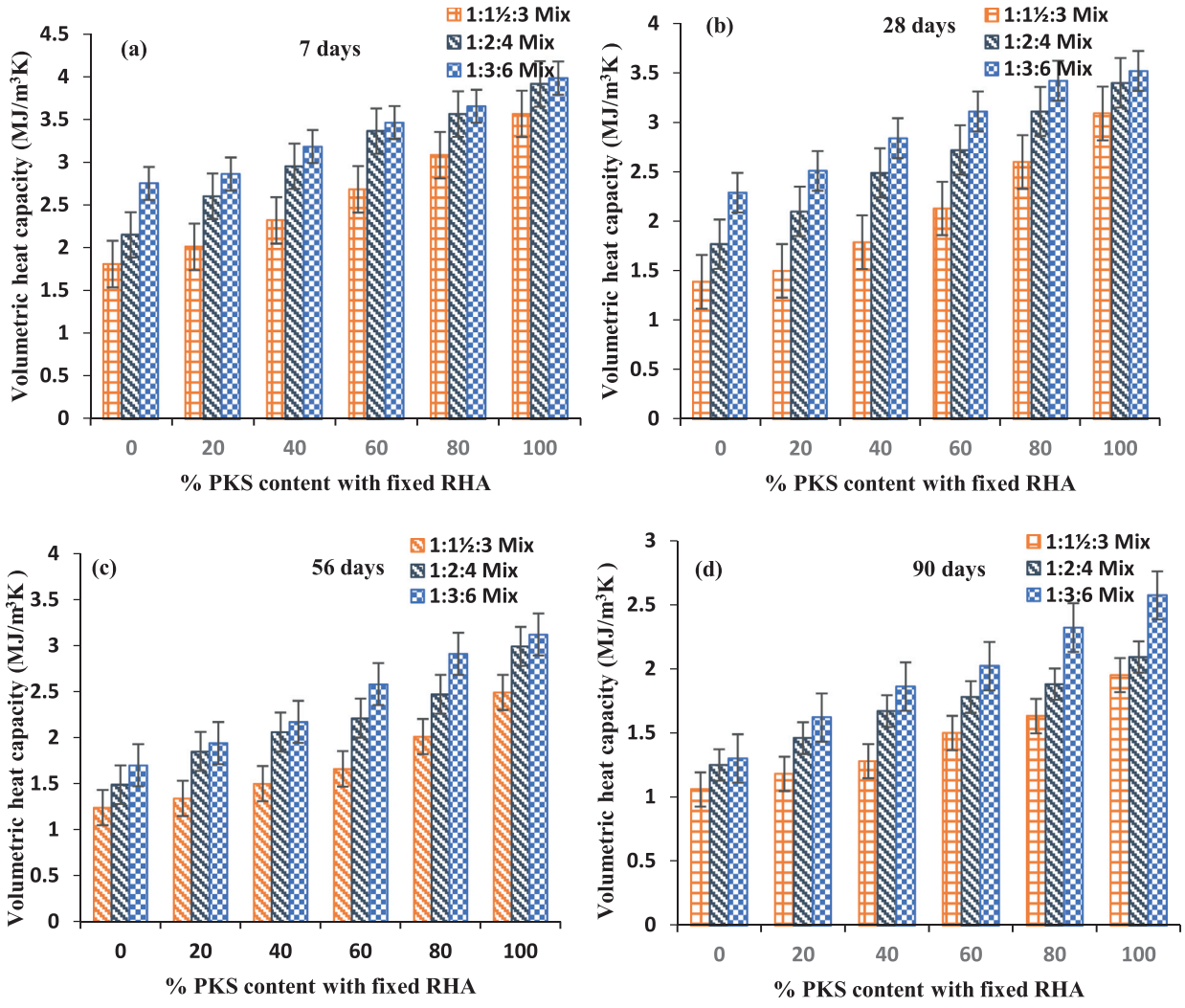


Fig. 11. Volumetric heat capacity of RHA-blended PKSC at: (a) 7 days; (b) 28 days; (c) 56 days; and (d) 90 days.

2021; Krishnaiah and Singh, 2006). Because of the porous nature and increased water absorption rate of these materials, the amount of energy required to increase a unit mass by one unit of temperature at constant pressure would increase. As a result, concrete's individual heat potential rises (Othuman Mydin, 2016), leading to the rise in volumetric heat capacity. The findings from the present study suggest that PKSC has a higher heat storage capacity, which will help thermal cycle balance between the building and its atmosphere, keeping residential and commercial buildings warm and lowering heating costs and CO_2 emissions. In the presence of RHA, this effect is amplified. This concrete form can be advantageous in terms of reducing the occurrence of temperature inside the structure according to Ocholi et al. (2014). This effect is enhanced in a presence of RHA. This concrete type could be of benefit for minimizing the incidence of temperature within the structure.

The presented results also indicated that the curing age had influence on volumetric heat capacity of RHA-blended PKSC as shown in Fig. 11. For example, the volumetric heat capacity decreased around 1.45–0.75 MJ/m^{3}K, 1.24–0.83 MJ/m^{3}K, 1.32–1.04 MJ/m^{3}K, 1.58–1.18 MJ/m^{3}K, 1.68–1.33 MJ/m^{3}K, 1.82–1.41 MJ/m^{3}K, for RHA-blended

PKSC with 0%, 20%, 40%, 60%, 80% and 100% aggregate replacement ratio, respectively as the curing age increased from 7 days to 90 days. This can be ascribed to the change in moisture content of concrete due to hydration of concrete with increase in curing ages. Thus, less heat is liberated (Nehdi and Soliman, 2011). This implies that additional hydration products are produced with increase in curing age thereby filling the concrete's voids (Ulykbanov et al., 2019). Thus, the concrete density increases and the volumetric heat capacity value decreases. A decline in volumetric heat capacity of concrete with age was also reported elsewhere (De Schutter and Taerwe, 1995; Bentur, 2003). In contrast to these findings, Raheem et al. (2015) found that as the curing age increased, the volumetric heat capacity of concrete with saw dust ash as a partial cement replacement increased. Huang et al. (2021) discovered that curing age had little or no effect on the volumetric heat capacity of OPC-based mortars.

As shown in Fig. 11, the volumetric heat capacity of RHA-blended PKSC is influenced by the aggregate/cement ratio in the three mix ratios. For example, the volumetric heat capacity of control concrete with 1:3:6 mix ratio having the highest aggregate/cement ratio was 0.6 MJ/m^{3}K and 0.94 MJ/m^{3}K higher than those with 1:1$\frac{1}{2}$:3 and 1:2:4, respectively. This indicates that the concrete with 1:3:6 mix ratio which had the lowest density had the highest volumetric heat capacity values followed by 1:2:4 and 1:1$\frac{1}{2}$:3 mix ratios. This corroborates with the findings from previous studies (Howlader et al., 2012), where the concrete with higher aggregate/cement ratio of 1:2:3 mix ratio which exhibited lower density exhibited higher specific heat capacity than the concrete with 1:1.5:2 mix ratio. This can be attributed to the change in filling paste ratio as a result of the rise of concrete porosity with increasing aggregate content and decreasing cement paste present in concrete mix (Ngohpok et al., 2018).

According to Tatro (2006) the specific heat capacity of CC range from 0.917 J/(gK) at 10 $^{\circ}$C to 1.038 J/(gK) at 66°C. The specific heat capacity values observed for concrete with 0–100% PKS substitution for the three mix ratios were below the minimum specified volumetric heat capacity value for CC.

Fig. 12 shows the correlation between the 28-day the volumetric heat capacity and oven-dry density of RHA-blended PKSC. As the inclusion of PKS increased, the oven-dry density of concrete decreased while the volumetric heat capacity increased and an correlation with a correlation coefficient (R^2 = 0.956) suggesting that a good prediction of the volumetric heat capacity from oven-dry density of RHA-blended PKSC was obtained. Similar relationship was presented by Oktay et al. (2015), where concrete incorporating LWAs such as pumice, expanded perlite and rubber at higher replacement ratio exhibited lower density and higher specific heat capacity than those at lower replacement ratio. Huang et al. (2021) on the other hand, showed a linear rise in volumetric heat capacity when oven-dry density of OPC-based mortars increased.

3.6. Thermal resistivity

The results of the thermal resistivity of RHA-blended PKSC with various mix ratios at 7, 28, 56 and 90 days are shown in Fig. 13. It can be observed that the trends of thermal resistivity of RHA-blended PKSC correspond to that of specific heat capacity but contrary to those of thermal conductivity and thermal diffusivity. The PKS substitution rate influences the thermal resistivity of RHA-blended PKSC, as shown in Fig. 13. As an example, the 28-day thermal resistivity of RHA-blended PKSC for 1:1$\frac{1}{2}$:3 mix ratio increased from 145 $^{\circ}$C.cm/W to 159 $^{\circ}$C.cm/W, 168 $^{\circ}$C.cm/W, 173 $^{\circ}$C.cm/W, 182 $^{\circ}$C.cm/W and 202 $^{\circ}$C.cm/W as the aggregate replacement ratio increased from 0%, 20%, 40%, 60%, 80% and 100%, respectively. A similar trend was found for RHA-blended PKSC with other mix ratios for different ages. These corroborate with the findings from a study (Ocholi et al., 2014), where it was found that the thermal resistivity for concrete with increase in the addition of rubber aggregate as substitute for NA. The increase in thermal resistivity can be ascribed to the increase in concrete voids and decrease in concrete density with the incorporation of PKS and RHA having higher porosity than the conventional materials. This observation is in agreement with a study (Krishnaiah and Singh, 2006), which found that thermal resistivity decreased as density increased and vice versa. According to Krishnaiah and Singh (2006) the presence of high content SiO_2 and low content of Al_2O_3 and Fe_2O_3 in a pozzolan (RHA in this case) compared with cement can also contributed to the higher thermal resistivity RHA-blended PKSC. The results from the current study suggest that concrete containing PKS will have a higher resistance to heat flow, making it a stronger insulator, and that this effect will be improved with the addition of RHA.

As shown in Fig. 13, the thermal resistivity of RHA-blended PKSC is also influenced by the curing age. From 7 days to 90 days, the volumetric heat capacity decreased around 86–62 $^{\circ}$C.cm/W, 86–57 $^{\circ}$C.cm/W, 92–64 $^{\circ}$C.cm/W, 90–67 $^{\circ}$C.cm/W, 84–77 $^{\circ}$C.cm/W, 79–70 $^{\circ}$C.cm/W, for RHA-blended PKSC at 0%, 20%, 40%, 60%, 80% and 100% PKS replacement, respectively. The rise in thermal resistivity can be ascribed to hydration-induced changes in concrete moisture content as curing ages increase. The additional hydration products filled up the concrete voids (Ulykbanov et al., 2019), resulting to the increase in concrete density with subsequent increase in thermal resistivity of concrete. Raheem et al. (2015) on the other hand, observed a decrease in thermal resistance as the curing age increased for saw dust ash blended cement mortar. The findings also showed that the aggregate/cement ratio had influence on thermal resistivity of RHA-blended PKSC. For example, the thermal conductivity of control concrete with 1:3:6 mix ratio having the highest aggregate/cement ratio was 42 $^{\circ}$C.cm/W and 29 $^{\circ}$C.cm/W higher than those with 1:1$\frac{1}{2}$:3 and 1:2:4, respectively. This implies that concrete with 1:3:6 mix ratio, which had the lowest density exhibited the highest thermal resistivity followed by 1:2:4 and 1:1$\frac{1}{2}$:3 mix ratios. This may be due to the inclusion of more aggregate in the mix ratio of 1:3:6 compared with 1:2:4 and 1:1$\frac{1}{2}$:3 mix ratios, resulting in a decrease in cement content of concrete. This observation could not be corroborated further since the thermal resistivity of concrete from various mix ratios has rarely been reported in previous studies.

Fig. 14 depicts the relationship between the thermal resistivity and oven-dry density of RHA-blended PKSC at 28 days. It can be seen that the oven-dry density of concrete decreased as the percentage of PKS increased, while the thermal resistivity increased, resulting in an correlation with a correlation coefficient (R^2 = 0.985), indicating that the volumetric heat capacity could be predicted accurately from the oven-dry density of RHA-blended PKSC. Furthermore, the findings of the study shown in Fig. 14 are consistent with those shown in Fig. 12, where the volumetric heat capacity has a an exponential relationship with the oven-dry density.

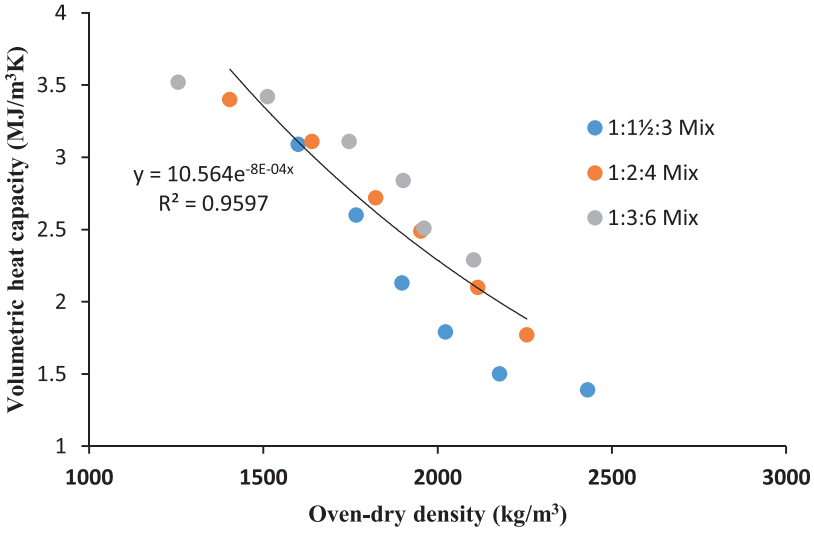


Fig. 12. Correlation between Oven-dry density and volumetric heat capacity.

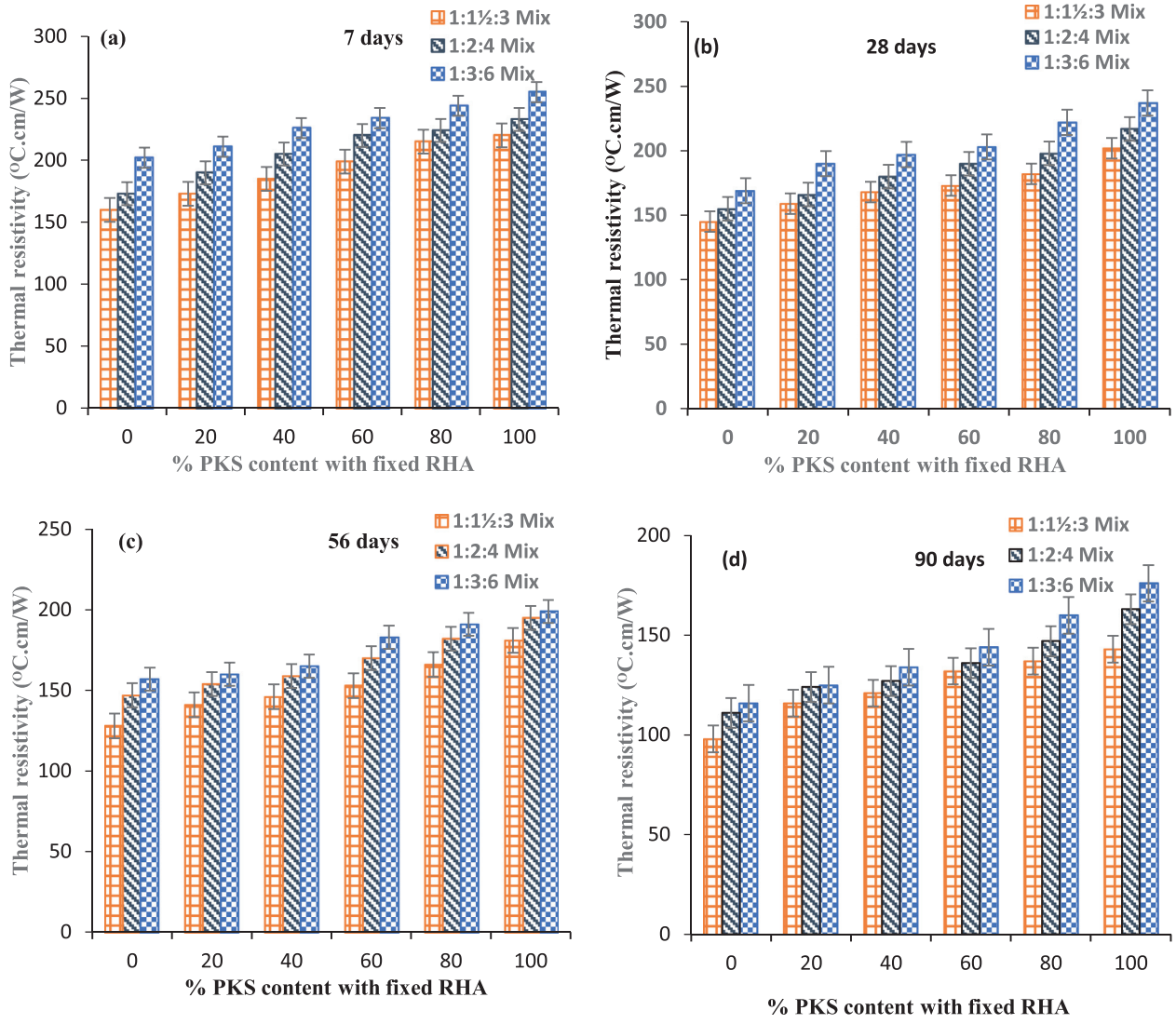


Fig. 13. Thermal resistivity of RHA-blended PKSC at: (a) 7 days; (b) 28 days; (c) 56 days; and (d) 90 days.

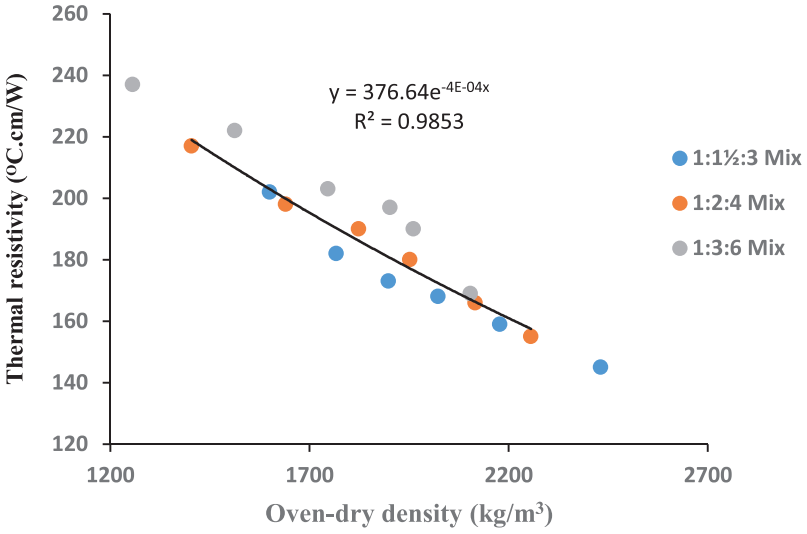


Fig. 14. Correlation between Oven-dry density and thermal resistivity.

Conclusions

The combined usage of PKS and RHA as alternative building materials for improving the thermal and insulation qualities of standard concrete was evaluated in this study. The design mixes used for concrete preparation were 1:1$\frac{1}{2}$:3, 1:2:4, 1:3:6 (cement: sand: granite/PKS) with w/c ratio of 0.5, 0.6 and 0.7, respectively. A fixed amount of RHA was used as a replacement for cement while PKS was used at varying substitute rate of NA. Concrete were tested in the laboratory for oven-dry density, compressive strength and thermal properties (thermal conductivity, thermal diffusivity, thermal resistivity, volumetric heat capacity). Based on the study's findings, the following conclusions were reached:

(i) Concrete density is reduced with the substitution of PKS for granite for all the mix ratios. Thus, the combination of RHA and PKS is suitable for producing lightweight concrete.

(ii) The compressive strength of concrete declined as the percentage of PKS increased but increased as the curing age increases. However, RHA-blended PKSC exhibited higher gain in strength than the control at the later age due to pozzolanic nature of RHA.

(iii) The RHA-blended PKSC failed to attain the targeted strength for mix ratio investigated. Conversely, the 40% PKS substitution for 1:1$\frac{1}{2}$:3 mix ratio and 20% PKS substitution for 1:2:4 mix ratio achieved the required strength for structural LWAC.

(iv) The thermal conductivity of concrete decreased as the amount of PKS and fixed RHA in the mix increased, and it increased with curing time. The 28-day thermal conductivity decreased from 1.61 to 0.53 W/mk for 1:1$\frac{1}{2}$:3 mix ratio; 1.32 to 0.48 W/mk for 1:2:4 mix ratio and 1.26 to 0.45 W/mk for 1:3:6 mix ratio at 0 to 100% PKS replacement. The concrete containing 40% PKS substitution and above for all the mix ratio attained the required thermal conductivity of LWAC useful for insulation purposes.

(v) Thermal diffusivity of concrete reduces with the addition of PKS and RHA and increase with curing age. The 28-day thermal diffusivity decreased from 0.60 to 0.37 mm/s^2 for 1:1$\frac{1}{2}$:3 mix ratio; 0.53 to 0.34 mm/s^2 for 1:2:4 mix ratio and 0.50 to 0.32 mm/s^2 for 1:3:6 mix ratio at 0 to 100% PKS replacement.

(vi) With the addition of PKS and RHA, concrete's volumetric heat capacity increases, and decline continues with increase in concrete ages. The 28-day thermal conductivity decreased from 1.39 to 3.09 MJ/m^{3}K for 1:1$\frac{1}{2}$:3 mix ratio; 1.77 to 3.40 MJ/m^{3}K for 1:2:4 mix ratio and 2.29 to 3.09 MJ/m^{3}K for 1:3:6 mix ratio at 0 to 100% PKS replacement.

(vii) Thermal resistivity of concrete increased as the amount of PKS and fixed RHA in the mix increased, and it decreased with curing time. The 28-day thermal conductivity decreased from 145 to 202 ^{O}C.cm/W for 1:1$\frac{1}{2}$:3 mix ratio; 155 to 217 ^{O}C.cm/W for 1:2:4 mix ratio and 169 to 237 ^{O}C.cm/W for 1:3:6 mix ratio at 0 to 100% PKS replacement.

(viii) The oven-dry bulk density was shown to have a significant correlation with thermal conductivity and compressive strength.

(ix) Concrete incorporating 40% PKS and 15% RHA for 1:1$\frac{1}{2}$:3 mix ratio achieved the compressive strength and thermal conductivity values specified for LWAC which is suitable for structural and insulation purposes. Thus, the concrete incorporating PKS and RHA is more beneficial in enhancing the thermal and insulating properties of structures with a largest energy savings than the CC.

Declaration of Competing Interest

The authors declare there are no conflicts of interest in this research.

References

CEMBUREAU, 2020. The role of cement in the 2050 low carbon economy. Eur. Cement Assoc. 1–64 http:/www.cembureau.cu/activity-report/(Accessed 6 June 2020).

Reddy, L.S.I., Vijayalakshmi, M.M., Praveenkumar, T.R., 2020. Thermal conductivity and strength properties of Nanosilica and GGBS incorporated concrete specimens. ed industrial waste reject. Silicon 1–12. doi:10.1007/s12633-020-00636-6.

Thakur, G., Asalam, M., Ganaoui, M.E., 2020. Energy efficient building envelope using waste PET in concrete. MATEC Web Conf. 307 01022, 1–5. doi:10.1051/matecconf/202030701022.

Shafigh, P., Azadi, I., Mahyuddin, N.B., 2018. Concrete as a thermal mass material for building applications - a review. J. Build. Eng. 19, 14–25. doi:10.1016/j.jobe.2018.04.021.

Misri, Z., Ibrahim, M.H.W., Awal, A.S.M.A., Desa, M.S.M., Ghadzali, N.S., 2018. Review on factors influencing thermal conductivity of concrete incorporating various type of waste materials. IOP Conf. Series: Earth Environ. Sci. 140, 012141. 10.1088/1755-1315/140/1/012141/202030701022.

Aurangzeb, A.Z., Gurmani, S.F., Maqsood, A., 2006. Simultaneous measurement of thermal conductivity, thermal diffusivity and prediction of effective thermal conductivity of porous consolidated igneous rocks at room temperature. J. Phys. D: Appl. Phys. 39, 3876–3881. doi:10.1088/0022-3727/39/17/025.

Howlader, M.K., Rashid, M.H., Mallick, D., Haque, T., 2012. Effects of aggregates types on thermal properties of concrete. ARPN J. Eng. Appl. Sci. 7, 900–906.

Asadi, I., Shafigh, P., Abu Hassan, Z.F.B., Mahyuddin, N.B., 2019. Thermal conductivity of concrete - a review. J. Build. Eng. doi:10.1016/j.jobe.2018.07.002.

Kodur, V.K.R., Sultan, M.A., 2003. Effect of temperature on thermal properties of high-strength concrete. J. Mater. Civ. Eng. 15, 101–107. doi:10.1061/(ASCE)0899-1561(2003)15:2(101).

International Energy Agency (IEA), https://www.iea.org/topics/buildings/, 2020 (Accessed 12 July 2021).

ACI 122R-14, Guide to thermal properties of concrete and masonry systems, American Concrete Institute 38800, country club drive, farmington hills, MI, 48331, USA. Detroit, pp.21, 2014.

Sengul, O., Azizi, S., Karaosmanoglu, F., Tasdemir, M.A., 2011. Effect of expanded perlite on the mechanical properties and thermal conductivity of lightweight concrete. Energy Build. 43, 671–676.

Li, Z., 2011. Advanced Concrete Technology. John Wiley and Sons, Inc., Canada.

Demirboğa, R., Gül, R., 2003. The effect of expanded perlite aggregate, silica fume and fly ash on the thermal conductivity of lightweight concrete. Cem. Concr. Res. 42, 349–354.

Skalny, J., Marchand, J., Odler, I., 2002. Sulfate Attack on Concrete. Taylor and Francis, London.

Real, S., Gomes, M.G., Rodrigues, A.M., Bogas, J.A., 2016. Contribution of structural lightweight aggregate concrete to the reduction of thermal bridging effect in buildings. Constr. Build. Mater. 121, 460–470.

Traore, Y.B., Messan, A., Hannawi, K., Gerard, J., Prince-Agbodjan, W., Tsobnang, F., 2017. Experimental investigations on the physical and mechanical properties of lightweight concrete using oil palm shell as coarse aggregate. J. Mater. Sci. Eng. A 7, 157–168.

Traore, Y.B., Messan, A., Hannawi, K., Gerard, J., Prince-Agbodjan, W., Tsobnang, F., 2018. Effect of oil palm shell treatment on the physical and mechanical properties of lightweight concrete. Constr. Build. Mater. 161, 452–460.

Raheem, A.A., Kareem, M.A., 2017. Chemical composition and physical characteristics of rice husk ash blended cement. Int. J. Eng. Res. Africa 32, 25–35. doi:10.4028/www.scientific.net/JERA.32.25.

Raheem, A.A., Nwakanma, E.O., Ogunleye, K.O., 2008. Engineering properties of concrete with palm kernel shell as fine and coarse aggregates. USEP: J. Res. Civil Eng. 5, 56–67.

Regin, J.J., Vincent, P., Ganapathy, C., 2016. Effect of mineral admixtures on mechanical properties and chemical resistance of lightweight coconut shell concrete. Arab J. Sci. Eng. 41, 1239–1242.

Aboshio, A., Shuaibu1, H.G., Abdulwahab, M.T., 2018. Properties of rice husk ash concrete with periwinkle shell as coarse aggregates. Niger. J. Technol. Devel. 15, 33–38.

Bahrami, A., Soltani, N., Pech-Canul, M.I., Gutiérrez, C.A., 2015. Development of metal-matrix composites from industrial/agricultural waste materials and their derivatives. Crit. Rev. Environ. Sci. Technol. 1–66. doi:10.1080/10643389.2015.1077067.

Food and Agricultural Organization (FAO), Records. http://fao.org/faostat/en/#data/QC/, 2018 (Accessed 9 September 2020).

Teo, D.C.L., Mannan, M.A., Kurian, V.J., 2006. Structural concrete using oil palm shell (OPS) as lightweight aggregate. Turk. J. Eng. Environ. Sci. 30, 251–257.

Okpala, D.C., 1990. Palm kernel shell as lightweight aggregate in concrete. Build. Environ. 25, 291–296.

Poku, K., 2002. Small-scale Palm Oil Processing in Africa, 148. FAO Agricultural services bulletin, Rome.

Alengaram, A.U., Al Muhit, B.A., Jumaat, M.Z., Michael, L.Y.J., 2013. A comparison of the thermal conductivity of oil palm shell foamed concrete with conventional materials. Mater. Des. 51, 522–529.

Serri, E., Suleiman, Md.Z., Md, A.Othuman Mydin, 2014a. The effects of oil palm shell aggregate shape on the thermal properties and density of concrete. Adv. Mater. Res. 935, 172–175.

Khan, M.I., 2002. Factors affecting the thermal properties of concrete and applicability of its prediction models. Build. Environ. 37, 607–614.

Demirboga, R., Türkmen, J., Karakoç, M.B., 2007. Thermo-mechanical properties of concrete containing high-volume mineral admixtures. Build. Environ. 723–727.

Raheem, A.A., Adesanya, D.A., 2011. A study of thermal conductivity of corn cob ash blended cement mortar. The Pacific J. Sci Tech. 12, 106–111.

Raheem, A.A., Oriola, K.O., Ismail, A., 2015. Investigating the thermal properties of sawdust ash-cement concrete as a potential construction material. LAUTECH J. Eng. Technol. 9, 91–100.

Huang, G., Pudasainee, D., Gupta, R., Liu, W.V., 2021. Thermal properties of calcium sulfoaluminate cement-based mortars incorporated with expanded perlite cured at cold temperatures. Constr. Build. Mater. 274, 1–13 122082.

Agricultural Market Information System (AMIS), Market monitor September 2021. Available at http://www.amis-outlook.org/, 2021 (accessed 7 September 2021).).

Thrive Agric, Statistics: rice production in Nigeria. https://medium.com/thrive-agric/rice-production-in-nigeria-7ef4918ced6a/, 2020 (accessed 7 September 2021).

Zerbino, R., Giaccio, G., Isaia, G.C., 2011. Concrete incorporating rice-husk ash without processing. Constr. Build. Mater. 25, 371–378.

Nilantha, B.G.P., Jiffry, I., Kumara, Y.S., Subashi, G.H.M.J., 2010. Structural and thermal performances of rice husk ash (RHA) based sand cement block. In: Proceedings of the International Conference on Sustainable Built Environment (ICSBE-2010), Kandy, pp. 138–144 13-14 December.

Soltani, N., Bahrami, M.I., Pech-Canul, L.A., 2014. Review on the physicochemical treatments of rice husk for production of advanced materials. Chem. Eng. J. doi:10.1016/j.cej.2014.11.056.

Silva, D., Pachla, E., Marangon, E., Tier, M., Garcia, A.P., 2020. Effects of rice husk ash and wollastonite incorporation on the physical and thermal properties of refractory ceramic composites. Revista Matéria 25, 1–10.

Jamil, M., Khan, M.N.N., Karim, M.R., Kaish, A.B.M.A., Zain, M.F.M., 2016. Physical and chemical contributions of rice husk ash on the properties of mortar. Constr. Build. Mater. 128, 185–198.

Filho, J.P., Garcez, M.R., Medeiros, M.H.F., Silva Filho, L.C.P., Isala, G.C., 2017. Reactivity assessment of residual rice-husk ashes. J. Mater. Civ. Eng. 04017003, 1–7.

Abalaka, A.E., 2013. Strength and some durability properties of concrete containing rice husk ash produced in a charcoal incineration at low specific surface. Int. J. Concr. Struct. Mater. 7, 287–293.

Rattanachu, P., Toolkasikorn, P., Tangchirapat, W., Chindaprasirt, P., Jaturapitakkul, C., 2020. Performance of recycled aggregate concrete with rice husk ash as cement binder. Cem. Concr. Comp. 108, 1–9 103533.

Chindaprasirt, P., Kanchanda, P., Sathonsaowaphak, A., Cao, H.T., 2007. Sulfate resistance of blended cements containing fly ash and rice husk ash. Constr. Build. Mater. 21, 1356–1361.

Bahrami, A., Simon, U., Soltani, N., Zavareh, S., Schmidt, J., Pech-Canul, M.I., Gurlo, A., 2016. Eco-fabrication of hierarchical porous silica monoliths by ice-templating of rice husk ash. Green Chem doi:10.1039/c6gc02153k.

Praveenkumar, T.R., Vijayalakshmi, M.M., Manigandan, S., 2019. Thermal Conductivity of Noval Reinforcement using TiO_2 Nanoaparticles and Rice Husk Ash. Int. J. Ambient Energy. doi:10.1080/01430750.2019.1691649.

Foong, K.Y., Alengaram, U.J., Jumaat, M.Z., 2015. Enhancement of the mechanical properties of lightweight oil palm shell concrete using rice husk ash and manufactured sand. J. -Zhejiang Univ. - Sci. A (Appl. Phys. Eng.) 16, 59–69.

Othuman Mydin, Md.A., 2016. Assessment of thermal conductivity, thermal diffusivity and specific heat capacity of lightweight aggregate foamed concrete. Jurnal Teknologi 78, 477–482.

Philips, E.S., Mutuku, R.N., Nwero, J.N., 2017. Effects of palm kernel shell and rice husk ash as partial replacements of normal weight aggregate and ordinary Portland cement in concrete. Eur. Int. J. Sci. Technol. 6, 42–52.

BS EN 197-1, Composition, specification and conformity criteria for common cements, British Standard Institute, 389 Chiswick high Road, London, W4 4AL. 2011.

Thong, C.C., Teo, D.C.L., Ng, C.K., 2017. Durability characteristics of polyvinyl alcohol–treated oil palm shell concrete. J. Mater. Civ. Eng. 29, 1–9.

ASTM C618-12, 2012. Standard Specification for Coal Fly Ash and Raw Calcined Natural Pozzolan for Use as a Mineral Admixture in Concrete. ASTM International, West Conshohocken, PA, USA.

Nguyen, C.V., 2021. Properties of locally-sourced rice husk ash (RHA)-blended mortar. J. Hunan Univ. (Nat. Sci.) 48, 63–75.

BS 1881-125, 2013. Method of Mixing and Sampling Fresh Concrete in the Laboratory. British Standard, London.

ASTM C642-13, 2013. Standard Test Method For density, Water Absorption and Voids in Hardened Concrete. ASTM International, West Conshohocken, PA, USA.

ASTM C39/C39M-12, 2012. Standard Test Method For Compressive Strength of Cylindrical Concrete Specimens, 4-2 Annual Book of ASTM Standard. Philadelphia.

ASTM D5334-14, 2014. Standard Test Method For Determination of Thermal Conductivity of Soil and Soft Rock by Thermal Needle Probe Procedure. ASTM International, West Conshohocken, PA, USA.

H.S. Carslaw, J.C. Jaeger, Conduction of Heat in Solids, 2nd Edition. Oxford, London, 1959.

Kluitenberg, G.J., Ham, J.M., Bristow, K.L., 1993. Error analysis of the heat pulse method for measuring soil volumetric heat capacity. Soil Sci. Soc. Am. J. 57, 1444–1451.

Sobuz, H.R., Hasan, N.Md.S., Tamanna, N., Islam, Md.S., 2014. Structural lightweight concrete production by using oil palm shell. J. Mater. 870247, 1–6. doi:10.1155/2014/870247.

Maghfouri, M., Shafigh, P., Aslam, M., 2018. Optimum oil palm shell content as coarse aggregate in concrete based on mechanical and durability properties. Adv. Mater. Sci. Eng. 4271497, 1–14. doi:10.1155/2018/4271497.

Damdelen, O., Georgopoulos, C., Limbachiya, M., 2014. Measuring thermal mass of sustainable concrete mixes. J. Civil Eng. Architech. 8, 213–220.

Newman, J., Owens, P., 2003. Properties of Lightweight Concrete, Advanced Concrete Technology Set. Butterworth-Heinemann, Oxford, UK.

Olanipekun, E.A., Olusola, K.O., Ata, O.A., 2006. A comparative study of concrete properties using coconut shell and palm kernel shell as coarse aggregates. Build. Environ. 41. doi:10.1016/j.buildenv.2005.01.029, 297-230.

Braga, M., de Brito, J., Veiga, M.R., 2014. Reduction of the cement content in mortars made with fine concrete aggregates. Mater. Struct. 47, 171–182. doi:10.1617/s11527-013-0053-1.

Kareem, M.A., Orogbade, O.O., Ibiwoye, E.O., Olasupo, N.O., 2021. The use of palm oil mill effluent as mixing and curing water in cement-based composite. Silicon 1–12. doi:10.1007/s12633-020-00864-w.

Djima, M.O.A., Mang'uriu, G.N., Mwero, J.N., 2018. Experimental investigation of lime treated palm kernel shell and sugarcane bagasse ash as partial replacement of coarse aggregate and cement respectively in concrete. Open J. Civ. Eng. 8, 358–372.

Azunna, S.U., 2019. Compressive strength of concrete with palm kernel shell as a partial replacement for coarse aggregate. SN Appl. Sci 1, 1–10. doi:10.1007/s42452-019-0334-6.

Osei, D.Y., Jackson, E.N., 2012. Experimental study on palm kernel shells as coarse aggregates in concrete. Int. J. Sci. Eng. Res. Civ. Eng. 5, 56–67.

Shafigh, P., Jumaat, M.Z., Mahmud, H.B., 2012. Effect of replacement of normal weight coarse aggregate with oil palm shell on properties of concrete. Arab J. Sci. Eng. 37, 955–964.

Ulykbanov, A., Sharafutdinov, E., Chung, C.-.W., Zhang, D., Shon, C.S., 2019. Performance-based model to predict thermal conductivity of non-autoclaved aerated concrete through linearization approach. Constr. Build. Mater. 196, 555–563. doi:10.1016/j.conbuildmat.2018.11.147.

Uysal, H., Demirboga, R., Sahin, R., Gül, R., 2004. The effect of different cement dosages, slumps and pumice aggregates ratios on the thermal conductivity and density of concrete. Cem. Concr. Res. 34, 845–848.

Chao-lung, H., Anh-Tuan, B.L., Chun-Tsun, C., 2011. Effect of rice husk ash on the strength and durability characteristics of concrete. Constr. Build. Mater. 25, 3768–3772. https://10.1016/j.conbuildmat.2011.04.0093.

BS EN 1992-1-1:2004+A1, 2014. Eurocode 2: Design of Concrete Structures- Part 1-1: General rules and Rules For Buildings. British Standards Institution, London.

ASTM C 330/C 330M, 2014. Standard Specification for Lightweight Aggregates for Structural Concrete. ASTM International, West Conshohocken, US.

ACI 213R-03, 2003. Guide for Structural Lightweight Aggregate Concrete, American Concrete Institute 38800. Country Club Drive, Farmington Hills, MI, 48331, USA.

Liu, W.V., Apel, D.B., Bindiganavile, V.S., 2014. Thermal properties of lightweight dry-mix shotcrete containing expanded perlite aggregate. Cem. Concr. Comp. 53, 44–51.

Serri, E., Mydin, Md.A.Othuman, Suleiman, Md.Z., 2014b. Thermal properties of oil palm shell lightweight concrete with different mix design. J. Teknol. 70, 155–159.
Kim, K.-.H., Jeon, S.E., Kim, J.-.K., Yang, S., 2003. An experimental study on thermal conductivity of concrete. Cem. Concr. Res. 33, 363–371.
Ngohpok, C., Sata, V., Satiennam, T., Klungboonkrong, P., Chindaprasirt, P., 2018. Mechanical properties, thermal conductivity, and sound absorption of pervious concrete containing recycled concrete and bottom ash aggregates. KSCE J. Civil Eng. 1–8.
Newman, J.B., 1993. Properties of structural lightweight aggregate concrete. Structural lightweight Aggregate Concrete J.L. Clarke (Eds). Blackie Academic & Professional, Glasgow, UK.
RILEM, Functional classification of lightweight concretes, Recommendation LC2, 2nd edition. 1978.
Oktay, H., Yanruta, S.R., Akpolat, A., 2015. Mechanical and thermophysical properties of lightweight aggregate concretes. Constr. Build. Mater. 96, 217–225.
Zulkarnain, F., Sulieman, Md.Z., Serri, E., 2014. The effect of mix design on mechanical and thermal properties of oil palm shell (OPS) lightweight concrete. J. Civ. Eng. Res. 4, 203–207.
Tandiroglu, A., 2010. Temperature-dependent thermal conductivity of high strength lightweight raw perlite aggregate concrete. Int. J. Thermophys. 31, 1195–1211.
Hossain, S.K.S., Mathur, L., Singh, P., Manjhi, M.J., 2017. Preparation of forsterite refractory using highly abundant amorphous rice husk silica for thermal insulation. J. Asian Ceram. Soc. doi:10.1016/j.jascer.2017.01.001.
Bentz, D.P., Peltz, M.A., Durán-Herrera, A., Valdez, P., Jua, C.A., 2011. Thermal properties of high-volume fly ash mortars and concretes. J. Build. Physics 34, 263–275. doi:10.1177/1744259110376613.
Hansen, P.F., Hansen, J., Hougaard, K., Pedersen, E.J., 1982. Thermal properties of hardening cement paste. In: Proceedings of RILEM International Conference on Concrete at Early Ages, RILEM, Paris, pp. 23–36.
Neville, A.M., 2008. Properties of Concrete, 14th ed Prentice Hall, Upper Saddle River, NJ, USA.
Krishnaiah, S., Singh, D.N., 2006. Determination of thermal properties of some supplementary cementing materials used in cement and concrete. Constr. Build. Mater. 20, 193–198.
Ocholi, A., Ejeh, S.P., Yinka, S.M., 2014. An investigation into the thermal performance of rubber-concrete. Acad. J. Interdiscipl. Stud. 3, 26–38.
Nehdi, M., Soliman, A.M., 2011. Early-age properties of concrete: overview of fundamental concepts and state-of-the art research. Constr. Mater. Proc. Inst. Civil Eng. doi:10.1680/coma.900040.
De Schutter, G., Taerwe, L., 1995. Specific heat and thermal diffusivity of hardening concrete. Mag. Concr. Res. 47, 203–208.
Bentur, A., 2003. (Ed.) Early-age cracking in cementitious systems. RILEM Technical Committee 181-EAS: early-age shrinkage induced stresses and cracking in cementitious systems. RILEM, Rep. 25, 335.
Tatro, S.B., 2006. Thermal properties. In: Significance of Tests and Properties of Concrete and Concrete-Making Materials STP 169D. ASTM International 100 Barr Harbour Drive West Conshoshocken, PA, pp. 226–237.